OPEN ACCESS Freely available online

PLOS ONE

The Paleoecology, Habitats, and Stratigraphic Range of the Enigmatic Cretaceous Brachiopod *Peregrinella*

Steffen Kiel[1]*, Johannes Glodny[2], Daniel Birgel[3], Luc G. Bulot[4], Kathleen A. Campbell[5], Christian Gaillard[6], Roberto Graziano[7], Andrzej Kaim[8], Iuliana Lazăr[9], Michael R. Sandy[10], Jörn Peckmann[3]

1 Georg-August-Universität Göttingen, Geowissenschaftliches Zentrum, Abteilung Geobiologie, Göttingen, Germany, **2** Deutsches GeoForschungsZentrum GFZ, Sektion 4.2, Anorganische und Isotopengeochemie, Telegrafenberg, Potsdam, Germany, **3** Universität Wien, Erdwissenschaftliches Zentrum, Department für Geodynamik und Sedimentologie, Wien, Austria, **4** FRE CNRS 2761, Centre de Sédimentologie-Paléontologie, Université de Provence, Marseille, France, **5** University of Auckland, Geology Programme, School of Environment Science, Auckland, New Zealand, **6** Université de Lyon-1, UMR CNRS 5125 Paléoenvironnements et Paléobiosphère, Villeurbanne, France, **7** Dipartimento di Scienze della Terra, dell'Ambiente e delle Risorse, Università di Napoli Federico II, Largo S. Marcellino, Napoli, Italia, **8** Instytut Paleobiologii PAN, Warszawa, Poland, **9** University of Bucharest, Faculty of Geology and Geophysics, Department of Geology, Bucharest, Romania, **10** University of Dayton, Department of Geology, Dayton, Ohio, United States of America

Abstract

Modern and Cenozoic deep-sea hydrothermal-vent and methane-seep communities are dominated by large tubeworms, bivalves and gastropods. In contrast, many Early Cretaceous seep communities were dominated by the largest Mesozoic rhynchonellid brachiopod, the dimerelloid *Peregrinella*, the paleoecologic and evolutionary traits of which are still poorly understood. We investigated the nature of *Peregrinella* based on 11 occurrences world wide and a literature survey. All *in situ* occurrences of *Peregrinella* were confirmed as methane-seep deposits, supporting the view that *Peregrinella* lived exclusively at methane seeps. Strontium isotope stratigraphy indicates that *Peregrinella* originated in the late Berriasian and disappeared after the early Hauterivian, giving it a geologic range of ca. 9.0 (+1.45/–0.85) million years. This range is similar to that of rhynchonellid brachiopod genera in general, and in this respect *Peregrinella* differs from seep-inhabiting mollusks, which have, on average, longer geologic ranges than marine mollusks in general. Furthermore, we found that (1) *Peregrinella* grew to larger sizes at passive continental margins than at active margins; (2) it grew to larger sizes at sites with diffusive seepage than at sites with advective fluid flow; (3) despite its commonly huge numerical abundance, its presence had no discernible impact on the diversity of other taxa at seep sites, including infaunal chemosymbiotic bivalves; and (4) neither its appearance nor its extinction coincides with those of other seep-restricted taxa or with global extinction events during the late Mesozoic. A preference of *Peregrinella* for diffusive seepage is inferred from the larger average sizes of *Peregrinella* at sites with more microcrystalline carbonate (micrite) and less seep cements. Because other seep-inhabiting brachiopods occur at sites where such cements are very abundant, we speculate that the various vent- and seep-inhabiting dimerelloid brachiopods since Devonian time may have adapted to these environments in more than one way.

Citation: Kiel S, Glodny J, Birgel D, Bulot LG, Campbell KA, et al. (2014) The Paleoecology, Habitats, and Stratigraphic Range of the Enigmatic Cretaceous Brachiopod *Peregrinella*. PLoS ONE 9(10): e109260. doi:10.1371/journal.pone.0109260

Editor: Matt Friedman, University of Oxford, United Kingdom

Received April 16, 2014; **Accepted** September 3, 2014; **Published** October 8, 2014

Data Availability: The authors confirm that all data underlying the findings are fully available without restriction. All relevant data are within the paper.

Funding: Financial support was provided by the Deutsche Forschungsgemeinschaft through grant Ki802/6-1 to SK; by the National Science Centre, Poland, through grant 2012/07/B/ST/10/04189 to AK; by the donors of the American Chemical Society – Petroleum Research Fund to MRS; and by the Open Access Publication Funds of the Georg-August-University Göttingen. The funders had no role in study design, data collection and analysis, decision to publish, or preparation of the manuscript.

Competing Interests: The authors have declared that no competing interests exist.

* Email: skiel@uni-goettingen.de

Introduction

The discovery of highly specialized animal communities around hydrothermal vents and methane seeps in the late 1970s and 1980s [1,2] and the question of their origin spurred the search for fossil examples of these ecosystems [3]. The major players of the modern, mollusk-dominated fauna, such as vesicomyid bivalves and bathymodiolin mussels, can be traced into the Eocene, and minor bivalve groups and various gastropods range into the Cretaceous [4–8]. In contrast, many Paleozoic and Mesozoic seep communities were dominated by organisms that are virtually absent from modern vents and seeps: rhynchonellid brachiopods [9]. Perhaps the most notable of these is the Early Cretaceous genus *Peregrinella* (Figure 1), the largest Mesozoic rhynchonellid brachiopod. *Peregrinella* long puzzled paleontologists because of its large size, its mass occurrence in isolated lenses and its widespread, yet disjunct, distribution [10–16].

Early in the 1980s various *Peregrinella* occurrences in the Vocontian basin in southern France were discussed as analogs to modern hydrothermal vent communities [17,18]. But it was only after the discovery of methane-seep communities in the Gulf of Mexico that *Peregrinella*-bearing deposits were identified as ancient methane seeps [19], based on stable carbon isotope analyses of a Californian example. These authors listed most occurrences of *Peregrinella* and noted that all are found as isolated

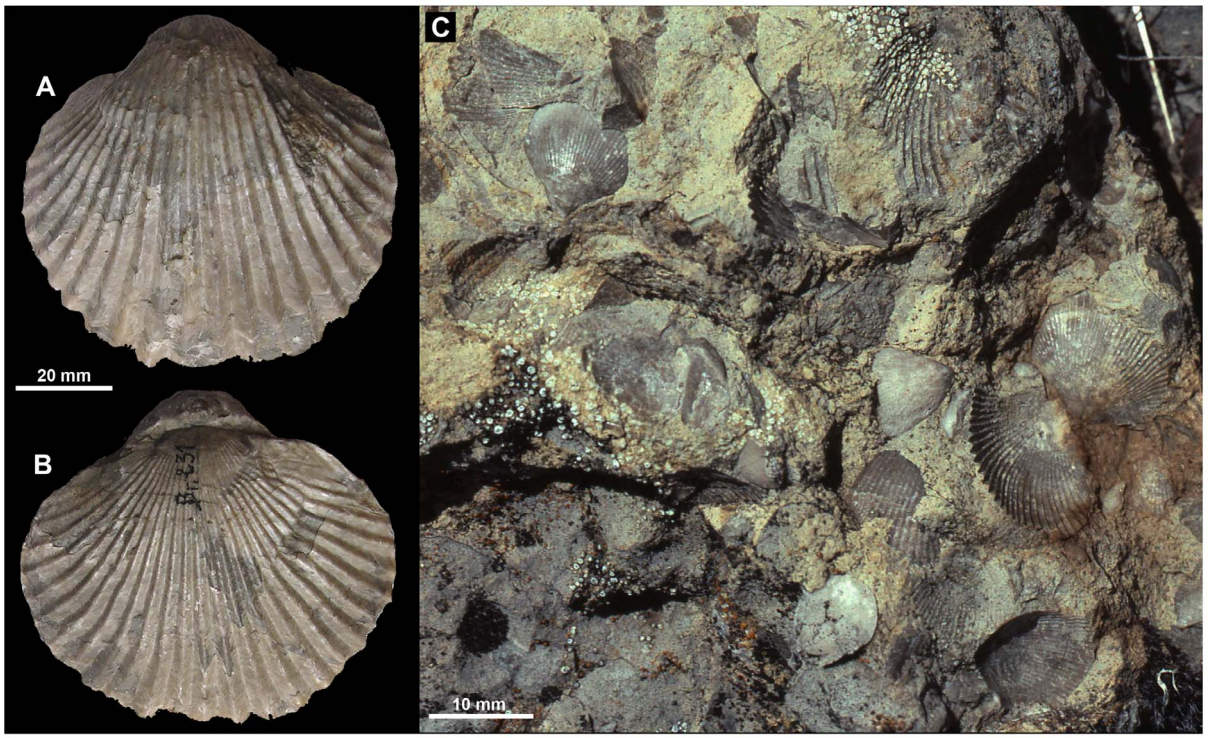

Figure 1. Examples of *Peregrinella*. A, B. *Peregrinella multicarinata* (Lamarck, 1819) from Rottier, southeastern France (EM 36190). C. Field image showing the mass occurrence of *Peregrinella whitneyi* (Gabb, 1866) at the Wilbur Springs seep site in California, USA.
doi:10.1371/journal.pone.0109260.g001

carbonate lenses within deep-water sediments similar to the Californian example. Therefore they suggested that *Peregrinella* lived exclusively at ancient methane seeps like the major taxa at vents and seeps today [19]. However, brachiopods are rare at modern vents and seeps and are only found in the marginal areas of these habitats. Thus, there are no modern analogs to the large and superabundant *Peregrinella* at fossil methane seeps (Figure 1C) and its paleoecologic and evolutionary traits remain poorly understood. Campbell and Bottjer [19] listed 18 occurrences world-wide, another one was subsequently reported from Alaska [20], and a summary of the biostratigraphic evidence for *Peregrinella* suggested a Berriasian to Hauterivian range for the genus [21].

Here we investigate strontium-isotope stratigraphy, petrography, stable carbon and oxygen isotopes, and the associated fauna of samples from 11 *Peregrinella* occurrences worldwide (Figure 2) that span its (suggested) stratigraphic range, together with a review of the available literature, to provide new insights into the nature of this enigmatic brachiopod. *Peregrinella* belongs to the superfamily Dimerelloidea, a clade that includes several seep-inhabiting or potentially seep-restricted brachiopods [22–27]: therefore, our results may have bearings on the role of brachiopods at vents and seeps throughout most of the Phanerozoic [9].

Material

Most localities sampled for this work have been described in detail elsewhere; here we just provide essential information and references in which further information can be found. The material is deposited in the Geowissenschaftliches Museum, Georg-August-Universität Göttingen, Germany (GZG), Institute of Paleobiology at the Polish Academy of Sciences, Warsaw, Poland (ZPAL), the collection of the Université Claude Bernard, Lyon-1, France (FSL) and the collection of the Ecole des Mines (EM) that is also housed at the Université Lyon-1, the University of Bucharest, Laboratory of Palaeontology, Romania (LPB), and the Smithsonian Natural History Museum, Washington, DC, USA (USNM).

Bonanza Creek (Alaska)

Peregrinella chisania shells are embedded in a carbonate matrix, a rather unusual lithology for the Chisana Formation that is composed mainly of volcanic rocks and mudstones and is considered as Valanginian-Hauterivian in age [20,28]. Two small specimens (USNM 487761 and 603602) were available for thin sectioning and isotope analyses (C, O, Sr).

Châtillon-en-Dois (France)

This locality in the Vocontian Basin is frequently mentioned in the literature on *Peregrinella* and was considered as Hauterivian in age [13,19,29], but the original locality has disappeared under urban development. A well-preserved shell was available for isotope analyses (C, O, Sr) from the collection of the Université Claude Bernard, Lyon-1 (FSL 425076).

Curnier (France)

A limestone block of about 1 m^3 with *Peregrinella multicarinata* was found as float in a dry creek near Curnier in southeastern France (coordinates: 44°23′23.4″N, 05°15′17.4″E). The associated macrofauna consists of the lucinid bivalve *Tehamatea vocontiana*, the gastropod *Humptulipsia macsotayi* [30], and various ammonites. Samples were collected by SK and LGB in 2010 and the material was used for thin sectioning, isotope analyses (C, O, Sr), and biomarker analysis (GZG.INV.82725-29). This occurrence was considered as Hauterivian in age [19].

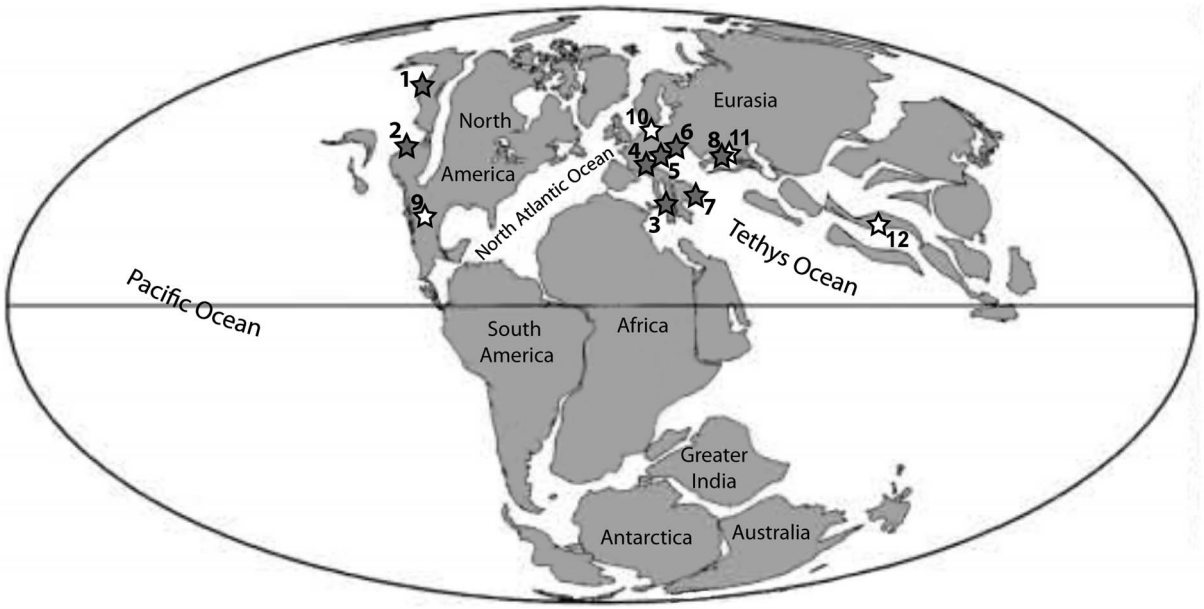

Figure 2. Distribution of the *Peregrinella* occurrences discussed herein, plotted on a paleogeographic map of the late Berriasian (140 m.y.a., [98]). Gray stars indicate occurrences for which new data are available: 1, Bonanaza Creek, Alaska; 2, Rice Valley and Wilbur Springs, California; 3, Incoronata, Italy; 4, Châtillon-en-Dois, Curnier and Rottier, southern France; 5, Musenalp, Switzerland; 6, Raciborsko, Poland; 7, Zizin Valley, Romania; 8, Planerskoje, Crimean peninsula. White stars indicate occurrences known from the literature: 9, Guanajuato seamount, Mexico; 10, Bohrung Werle, northern Germany; 11, Kuban, Russia; 12, Xainza County, Tibet.
doi:10.1371/journal.pone.0109260.g002

Incoronata (Italy)

Abundant material was collected in 2011 by SK and RG at the base of the Maiolica Formation, which onlaps the flank of the Apulia carbonate platform near the village of Mattinata on the Gargano promontory in southeastern Italy (coordinates: 41°43'25.8"N, 16°02'29.2"E), and was used for thin sectioning and isotope analyses (C, O, Sr; GZG.INV.82745, 46, 54). The locality and its geologic setting have been described elsewhere and the age of the *Peregrinella*-bearing sediments was considered as latest Valanginian-Early Hauterivian (*NC4a* Subzone) [31–33].

Musenalp (Switzerland)

A small block (30×20×20 cm) with abundant *Peregrinella subsilvana* was found about 10 m NE of the Schwändi hut (coordinates 46°56'26.4"N, 8°27'13.5"E) by SK in 2010, and was used for thin sectioning, isotope analyses (C, O, Sr), and biomarker analysis (GZG.INV.82730-38). The scattered *Peregrinella*-bearing blocks on the small and steep pasture around the Schwändi hut are from a nappe of the Préalpes Médianes and are derived from a post-glacial landslide [14]. This site was previously considered as the oldest occurrence of *Peregrinella*, being possibly of late Berriasian age [34].

Planerskoje (Crimean peninsula)

An isolated carbonate lens with *Peregrinella multicarinata* was found within well-bedded mudstone of the Planerskoje section in the southeastern Crimean peninsula (coordinates: 44°58'08.1"N, 35°12'01.5"E), considered as Hauterivian in age [35], and was sampled by SK in 2007. The petrography, stable isotopes, biomarkers, and fauna of this locality have been described in detail elsewhere [35–37]; here we investigate oxygen and strontium isotopes of *Peregrinella* shells (GZG.INV.82739-44).

Raciborsko (Poland)

Isolated, pyrite-rich carbonate blocks with *Peregrinella multicarinata* occur within dark, marly shales of the Grodziszcze beds in the Silesian unit in the western Carpathians, considered as being of 'middle Neocomian' age [13]. Despite various efforts, this locality has not been re-located in recent years but several small specimens of Biernat's collection (ZPAL Bp.III) at the Institute of Paleobiology at the Polish Academy of Sciences, Warsaw, were available for thin sectioning and isotope analyses (C, O, Sr).

Rice Valley (California)

Isolated limestone lenses with *Peregrinella whitneyi* occur within the Rice Valley outlier of the Great Valley Group in Lake County, California, USA [38]; approximate coordinates: 39°21′02″N, 122°52′01″W). A hand sample collected by KAC was used for thin sectioning, and isotope analyses (C, O, Sr) of *Peregrinella* shells (GZG.INV.82747-52).

Rottier (France)

Peregrinella-bearing limestone crops out near the village of Rottier in southeastern France [29] and were sampled by SK and CG in 2006 and by SK and LGB in 2010, but only a few *Peregrinella* specimens were found. Additional *Peregrinella*-rich material for thin sectioning and isotope analyses (C, O, Sr) was selected from the collection of the Université Claude Bernard, Lyon-1 (FSL 425077-79).

Wilbur Springs (California)

This is a large, isolated carbonate lens with *Peregrinella whitneyi* enclosed in serpentinite of the Great Valley Group. The petrography, stable isotopes, biomarkers and fauna of this locality have been described in detail elsewhere [39–41]. Its age was considered as Valanginian in the older literature but more recently as Hauterivian [19]. A hand sample collected by KAC was used

for thin sectioning and for isotope analyses (C, O, Sr) of *Peregrinella* shells (GZG.INV.82753, 82755, 82756); four specimens from the USNM collection were used for stable C and O isotope analyses of *Peregrinella* shells (USNM 603596-603599).

Zizin Valley (Romania)

Shells of *Peregrinella multicarinata* are found here both within isolated carbonate blocks as well as scattered through the surrounding flysch deposits of the Sinaia Formation, which is reportedly of late Hauterivian to early Barremian age [12,42]. The *Peregrinella*-bearing carbonates were identified as seep deposits using petrographic, stable isotope, and biomarker investigations [42]. Shells from both types of occurrence were used for isotope analyses (C, O, Sr).

Two shells from active methane seeps in the northern Gulf of Mexico were available for comparative Sr isotope work, one of the bathymodiolin mussel "*Bathymodiolus*" *childressi* collected at brine pool NR-1 (site GC233) in 640 m depth [43], and one of a terebratulid brachiopod, *Ecnomiosa gerda*? Cooper, from Garden Banks block 647 in about 950–1000 m depth [44]. Specimens of a putative *Peregrinella* from a drill core in northeastern Germany [45] were also investigated, but their affinity to *Peregrinella* is questionable.

Methods

Thin sections of ca. 60 micrometer thickness were produced from the available material and the surfaces of the counterparts were polished to facilitate the selection of sampling sites for isotope analyses. Samples for stable carbon and oxygen isotope analyses were extracted either from the counterparts of the thin sections or from the brachiopod shells using a hand-held microdrill. Carbonate powders were reacted with 100% phosphoric acid at 75°C using a Finnigan Kiel IV Carbonate Device attached to a Finnigan DELTA V PLUS mass spectrometer. All values are reported in per mil relative to the PDB standard by assigning a $\delta^{13}C$ value of +1.95‰ and a $\delta^{18}O$ value of −2.20‰ to NBS19. Reproducibility was checked by replicate analysis of laboratory standards and is better than ±0.05‰. Paleotemperatures were calculated from the $\delta^{18}O$ values of *Peregrinella* shells using the formula provided by [46] and assuming an ice-free ocean with a $\delta^{18}O_{seawater}$ value of −1.2. [47] and ignoring artifacts that were possibly introduced due to isotope exchange during late diagenesis and rock alteration.

For strontium isotopes we analyzed two different *Peregrinella* shells (where available) from each locality listed in the 'Material' section to check for potential inhomogeneity, distributed alteration or recrystallization of the original calcite. The microstructure of shell fragments was examined optically and with scanning electron microscopy (LEO 1530 SEM at 3.8 KV; specimens coated with 14 nm of platinum: Figure 3) to check for possible diagenetic alteration or intergrowth with siliciclastic material. Fragments devoid of any indications of recrystallization or contamination were selected and cleaned in distilled water and in pure ethanol. Wherever feasible we also cleaned the fragments by rinsing them in 1 N HCl for about 5 seconds to remove any secondary calcareous material and contaminants [48–50]. After another rinse in ultrapure water the shell fragments were dissolved in 2.5 N HCl. Strontium was isolated and recovered from the solutes by ion exchange using Dowex AG-50 cation exchange resin.

Mass spectrometry analyses of Sr isotopic compositions were carried out at GFZ Potsdam, using a Thermo-Finnigan Triton TIMS (thermal ionization mass spectrometry) instrument. Strontium was analyzed in dynamic multicollection mode. For the duration of the study, the mean value obtained for $^{87}Sr/^{86}Sr$ of the NBS standard SRM 987 (now NIST 987) was 0.710261±0.000006 (n = 10, 2σ SD). The $^{87}Sr/^{86}Sr$ value for SRM 987 used for construction of the LOWESS dataset for conversion of Sr isotope data into ages is 0.710248 [51], which requires application of a normalization factor of 0.999982 for our Sr isotope ratio data. Calculation of ages and age errors was performed using the 'Look-Up Table Version 5: 04/13' [52]. The error intervals calculated for our Sr isotope stratigraphy age data (see Table 1) are based on typical 2σ absolute uncertainties for single-analysis, first-measurement $^{87}Sr/^{86}Sr$ values of ±0.000020. This uncertainty is estimated from the overall analytical range of values obtained for the NBS standard SRM 987. The only exception is sample PS1804. Here we used the measured $2\sigma_m$ uncertainty since it was, because of small sample size, slightly higher than the standard-derived uncertainty. Analytical blanks for Sr are regarded negligible compared to the amounts of sample Sr in each analysis; hence, no blank correction was applied. To check for possible radiogenic in-growth of ^{87}Sr after shell deposition, we analyzed a few samples for Rb concentrations using a Thermo-Neptune multicollection ICP-MS instrument (GFZ Potsdam). Rubidium concentrations in the carbonate material are very low, in the range of less than 30 ppb. With typical Sr concentrations of at least several hundred ppm in both recent and fossil shell material (compilation of data in [53,54]), Rb/Sr ratios are low enough to rule out any significant post-depositional radiogenic in-growth of ^{87}Sr since shell growth.

For biomarker analysis, limestone samples from Curnier and Musenalp were prepared and decalcified after a method described previously [40]. After saponification with 6% potassium hydroxide in methanol, the samples were extracted with a microwave extraction system (CEM Discovery) at 80°C and a maximum of 250 W with a mixture of dichloromethane:methanol (3:1). The resulting total lipid extracts were pre-separated into an *n*-hexane soluble and dichloromethane soluble fraction. For further separation of the *n*-hexane fraction by column chromatography, the samples were separated into four fractions of increasing polarity [55]. Only the hydrocarbon fractions were found to contain indigenous compounds. The polar fractions did not yield genuine lipid biomarker patterns, and were found to be severely affected by thermal maturation and biodegradation. Hydrocarbon fractions were analyzed by coupled gas chromatography- mass spectrometry (GC-MS) with an Agilent 7890 A GC system coupled to an Agilent 5975 C inert MSD mass spectrometer at the Department of Geodynamics and Sedimentology, University of Vienna. The GC-MS was equipped with a 30 m HP-5 MS UI fused silica capillary column (0.25 mm i.d., 0.25 µm film thickness). The carrier gas was helium. The GC temperature program was as follows: 60°C (1 min); from 60°C to 150°C at 10°C/min; from 150°C to 320°C at 4°C/min, 25 min isothermal. Identification of compounds was based on retention times and published mass spectral data. Compound-specific carbon isotope analysis was performed with a Thermo Fisher Trace GC Ultra connected via a Thermo Fisher GC Isolink interface to a Thermo Fisher Delta V Advantage spectrometer at the Department of Terrestrial Ecosystem Research, University of Vienna. Conditions for gas chromatography were the same as described above. Stable carbon isotopic compositions are given as δ values in per mil relative to the PDB standard. Each measurement was calibrated using several pulses of carbon dioxide with known isotopic composition at the beginning and the end of the run. Instrument precision was checked with a mixture of *n*-alkanes (C_{14} to C_{38}) of known isotopic composition. Analytical standard deviation was below 0.9‰.

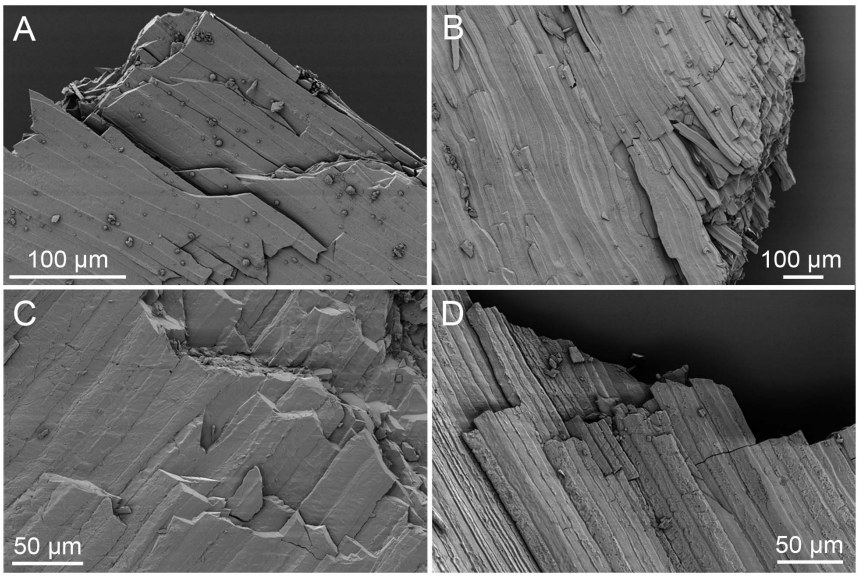

Figure 3. SEM images of well preserved *Peregrinella* shells with unaltered shell microstructure. The examples are from: A: Incoronata (GZG.INV.82745); B: Planerskoje (GZG.INV.82739); C: Musenalp (GZG.INV.82737); D: Curnier (FSL 425078).
doi:10.1371/journal.pone.0109260.g003

Statistic analyses of faunal data were conducted using the software package PAST v. 2.13 [56].

Sr-Isotope Stratigraphy of *Peregrinella* Occurrences

Using strontium isotope ratios to correlate the Sr isotopic signature of marine fossils with the global Sr seawater evolution curve [52], we dated the available *Peregrinella* occurrences. As outlined above, the sample preparation procedure was such that alteration or contamination of the analyzed samples is highly unlikely, so that the $^{87}Sr/^{86}Sr$ ratios obtained herein can reliably be converted into Sr isotope stratigraphic ages. Reliability of the calculated ages is also supported by the observation that pairs of two independent analyses of different shells from one locality in all cases revealed consistent results (Table 1).

Because all known occurrences of *Peregrinella* are Early Cretaceous (145.0 to 100.5 Ma) in age, we focused on the Early Cretaceous Sr seawater evolution curve. For the Early Cretaceous the Sr seawater evolution curve displays two maxima and one marked minimum (Figure 4), therefore, a specific Sr isotopic composition may correspond to different stratigraphic ages, and age determinations may be ambiguous. To resolve this ambiguity, we used available biostratigraphic and geologic information from the individual *Peregrinella* occurrences to constrain the definite Sr isotope stratigraphic ages. Results, including Sr isotopic compositions of specific samples and their corresponding ages, are presented in Table 1. For comparison, we also present Sr isotopic data on Recent shells of a terebratulid brachiopod and of the mussel "*Bathymodiolus*" *childressi* from methane seeps in the Gulf of Mexico, which are, as expected, indistinguishable from today's Sr seawater composition ($^{87}Sr/^{86}Sr = 0.709175$, [52]). This is important because the Sr-isotope signature of the seeping fluids at these sites often differs substantially from that of seawater [57,58] and it shows that mollusks and brachiopods incorporate the seawater Sr isotope signature in their shells, not that of the seeping fluids. Therefore we assume that the Sr-isotope signature in the shells of *Peregrinella* reflects that of the seawater in which they lived.

The Sr-isotope ages of two of the fossil sites that are biostratigraphically well-dated are in agreement with biostratigraphy. In particular, the occurrence at the Swiss Musenalp was dated as late Berriasian using tintinnids (calpionellids) [34], consistent with its Sr-isotope age [141.20 (+1.45/−1.20) Ma]; the occurrence at Rottier, France, was dated as early Hauterivian (Jeannoti-zone) using ammonites [29], consistent with its Sr-isotope age [132.20 (+0.60/−0.85) Ma] (Table 1).

Of interest is the Sr-isotope age of the Romanian occurrence in the Sinaia Formation. *Peregrinella* shells from this formation were transported, deriving from turbidites or isolated, allochthonous blocks of limestone enclosed in deep-water strata. These *Peregrinella*-bearing rocks were considered the geologically youngest occurrence, ranging into the early Barremian. This inference, however, was based on foraminifera from the surrounding mudstone of the Sinaia Formation, not from the *Peregrinella* limestone itself. Both investigated shells from this site, one from a carbonate, the other from a siltstone, yielded Sr-isotope values of 0.707379 to 0.707386, indicating a latest Valanginian to earliest Hauterivian age [133.70 (+2.25/−0.70) to 134.15 (+2.35/−0.95) Ma]. Therefore, it seems likely that the Romanian *Peregrinella* shells were eroded from their original latest Valanginian to earliest Hauterivian sediments and reworked into the late Hauterivian-early Barremian Sinaia Formation. The two younger ages that could also be derived from the measured Sr-isotope ratios (123 Ma, early Aptian, and 109 Ma, mid-Albian; see Table 1) can be ruled out because they are younger than the biostratigraphic age of the Sinaia Formation.

The Californian *Peregrinella whitneyi* at Wilbur Springs was considered as Valanginian in the earlier literature [13,21,59,60], but more recently a Hauterivian age was suggested due to the position of the locality just above the last occurrence of the index fossil *Buchia pacifica* [19]. Our Sr isotope data indicate a latest Valanginian to earliest Hauterivian age [133.20 (+0.95/−0.65) to 134.40 (+2.30/−1.10) Ma].

Table 1. Sr-isotope data and possible stratigraphic ages derived from the LOWESS 5.0 curve [52].

Sample	$^{87}Sr/^{86}Sr$ $\pm 2\sigma_m$ meas.	$^{87}Sr/^{86}Sr$ norm.	age 1 ($\pm 2\sigma$) (in Ma)	age 2 ($\pm 2\sigma$) (in Ma)	age 3 ($\pm 2\sigma$) (in Ma)
Bonanza Creek, Alaska (USNM 603602)	0.707416+/−0.000028	0.707403	**133.20** (+1.85/−0.95)	**125.40** (+1.10/−1.25)	**108.90** (+1.90/−>6.65
Bonanza Creek, Alaska (USNM 487761)	0.707437+/−0.000017	0.707424	**132.60** (+0.70/−0.60)	**126.10** (+0.80/−0.85)	(**104.05** or **96.65**)
Chatillon, France (FSL 425076)	0.707414+/−0.000005	0.707401	**133.25** (+1.10/−0.65)	**125.30** (+0.90/−0.90)	**109.10** (+1.50/−5.70)
Chatillon, France (FSL 425076)	0.707447+/−0.000005	0.707434	**132.40** (+0.60/−0.80)	**126.40** (+0.80/−0.75)	**approx. 100**
Curnier, France (GZG.INV.82729)	0.707440+/−0.000016	0.707427	**132.55** (+0.65/−0.65)	**126.20** (+0.80/−0.80)	(**103.30** or **97.00**)
Incoronata, Italy (GZG.INV.82745)	0.707365+/−0.000006	0.707352	**136.70** (+1.20/−2.40)	**123.30** (+1.00/−1.40)	**111.25** (+0.80/−0.95)
Incoronata, Italy (GZG.INV.82746)	0.707363+/−0.000006	0.707350	**136.80** (+1.20/−2.20)	**123.20** (+1.05/−1.40)	**111.30** (+0.80/−0.95)
Musenalp, Switzerland (GZG.INV.82737)	0.707271+/−0.000007	0.707258	**141.15** (+1.45/−1.20)	**117.50** (+1.75/−1.15)	**113.50** (+0.65/−0.55)
Musenalp, Switzerland (GZG.INV.82738)	0.707270+/−0.000004	0.707257	**141.20** (+1.45/−1.20)	**117.45** (+1.75/−1.15)	**113.50** (+0.65/−0.55)
Planerskoje, Crimea (GZG.INV.82739)	0.707298+/−0.000005	0.707285	**139.75** (+1.25/−1.05)	**119.10** (+1.60/−1.85)	**113.00** (+0.60/−0.65)
Planerskoje, Crimea (GZG.INV.82740)	0.707293+/−0.000007	0.707280	**140.00** (+1.30/−1.05)	**118.75** (+1.65/−1.65)	**113.10** (+0.60/−0.65)
Raciborsko, Poland (ZPAL Bp.III)	0.707399+/−0.000007	0.707386	**133.70** (+2.25/−0.70)	**124.70** (+1.00/−0.90)	**110.05** (+1.05/−4.70)
Rice Valley, California (GZG.INV.82747)	0.707387+/−0.000007	0.707374	**134.65** (+2.15/−1.30)	**124.25** (+0.95/−1.00)	**110.55** (+0.90/−1.55)
Rottier, France (FSL 425077)	0.707454+/−0.000008	0.707441	**132.20** (+0.60/−0.85)	**126.65** (+0.85/−0.75)	
Wilbur Springs, California (GZG.INV. 82755)	0.707389+/−0.000013	0.707376	**134.40** (+2.30/−1.10)	**124.30** (+0.95/−0.95)	**110.45** (+0.95/−1.70)
Wilbur Springs, California (GZG.INV. 82756)	0.707417+/−0.000009	0.707404	**133.20** (+0.95/−0.65)	**125.45** (+0.80/−0.95)	**108.80** (+1.70/−6.00)
Zizin Valley, Romania (LPB III br 387)	0.707392+/−0.000006	0.707379	**134.15** (+2.35/−0.95)	**124.45** (+0.95/−0.95)	**110.35** (+0.95/−2.25)
Zizin Valley, Romania (LPB III br 385)	0.707399+/−0.000005	0.707386	**133.70** (+2.25/−0.70)	**124.70** (+1.00/−0.90)	**110.05** (+1.05/−4.70)
"*Bathymodiolus*" *childressi*, Gulf of Mexico (GZG.INV.82764)	0.709189+/−0.000004	0.709176	**0.00** (+0.65/−0.00)		
Ecnomiosa gerda?, Gulf of Mexico (GZG.INV.82765)	0.709170+/−0.000008	0.709157	**0.55** (+0.45/−0.55)		
Ecnomiosa gerda?, Gulf of Mexico	0.709181+/−0.000004	0.709168	**0.24** (+0.58/−0.24)		

'age 1' are the ages that fall within the biostratigraphically possible age range, as also shown on Figure 4.
doi:10.1371/journal.pone.0109260.t001

A Hauterivian age was suggested for the occurrence in Rice Valley, California, based on the presence of *Peregrinella whitneyi* and a mollusk assemblage that is now known from many Early Cretaceous seep deposits in California [38]. The Sr-isotope age of this locality [134.65 (+2.15/−1.30) Ma (Table 1)] indicates a latest Valanginian age, similar to the Wilbur Springs site mentioned above. The sediments directly overlying the *Peregrinella*-bearing unit at Rice Valley are dated as Albian-Cenomanian based on palynomorphs [38], thus ruling out the equally consistent Albian Sr-isotope age (Table 1). However, we cannot entirely discard the equally consistent early Aptian Sr-isotope age, but the Hauterivian age is more likely because two of the mollusk species present in the Rice Valley seep carbonate (*Paskentana paskentaensis* and *Retiskenea*? *tuberculata*) are known from other Valanginian-Hauterivian seep deposits, but an Aptian seep deposit from this area (Cold Fork of Cottonwood Creek) contains a different set of taxa [41,61].

The Polish *Peregrinella* site at Raciborsko is situated roughly at the boundary between the Grodziszcze and Wierzowice (Verovice) shales in the Silesian Nappe and was considered as 'Neocomian' [13]. The age of this boundary is diachronous, being oldest (Hauterivian) in the west and becoming younger (as young as Aptian) in the east [62]. Raciborsko is located in the western part of the Silesian Nappe, and our Sr isotope data indicate a basal Hauterivian age for this locality [133.70 (+2.25/−0.70) Ma], consistent with its geographic location.

The Alaskan species *Peregrinella chisania* was previously considered as Valanginian-Hauterivian [20]; the Sr isotope data indicate an early Hauterivian age [133.20 (+1.85/−0.95) to 132.60 (+0.70/−0.60) Ma]. Because the Chisana Formation, from which the species name *P. chisania* is derived, hosts Valanginian to Barremian bivalves [28], the equally possible younger (early Aptian and Albian, see Table 1) Sr-isotope ages can be ruled out.

In summary, our Sr-isotope stratigraphic investigation confirms the so far oldest and youngest biostratigraphically well-dated occurrences as late Berriasian and early Hauterivian, respectively. It also shows that some occurrences of *Peregrinella* are slightly older than previously considered, but still within the range late Berriasian–late Hauterivian. Furthermore, it is evident that *Peregrinella* shells and even *Peregrinella*–bearing carbonate blocks can be reworked from their original sediment into younger sediments. Finally, we can refine ages of previously poorly dated occurrences (those dated as Valanginian-Hauterivian or 'Neocomian'), and show that they are confined within the range late Berriasian–late Hauterivian. An occurrence of *Peregrinella* possibly as young as Albian was reported from sediments of the Guanajuato seamount, central Mexico, an age that was based on co-occurring, reworked fossils of 'Neocomian' to Albian age [63]. However, considering that all specimens investigated here are of 'Neocomian' age and that the Romanian example documented here indicates that *Peregrinella* can be reworked into younger sediments, it seems likely that also the Mexican occurrence falls within the stratigraphic interval of the other localities, rather than being of Albian age. Thus, *Peregrinella* originated in the late Berriasian and most likely became extinct at the end of the early Hauterivian, giving it a geologic range of 9.0 (+1.45/−0.85)

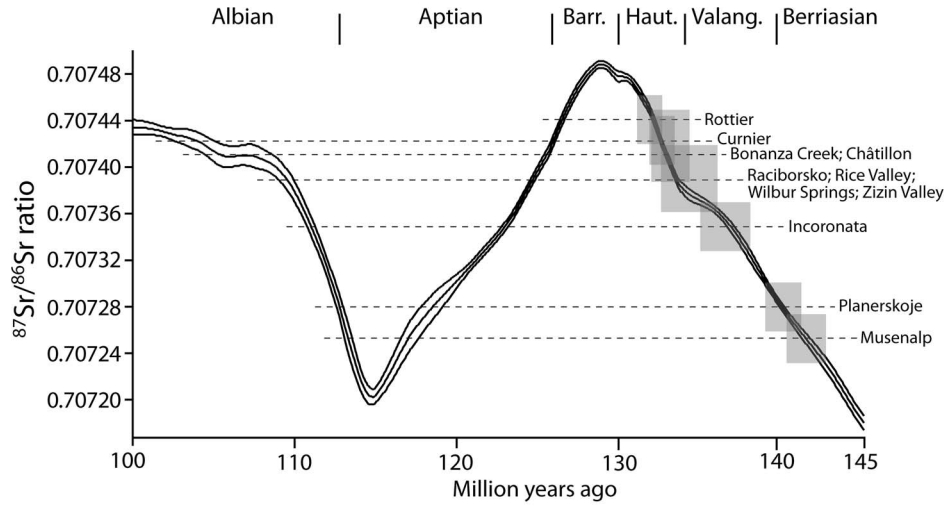

Figure 4. Strontium isotope curve for the Early Cretaceous and its upper and lower confidence interval [52]. Dashed lines indicate our measurements on *Peregrinella* shells; shaded areas indicate the error margins (vertical: Sr isotope ratio; horizontal: geologic age) of those ages that fall within the biostratigraphically possible age range.
doi:10.1371/journal.pone.0109260.g004

million years according to the Gradstein et al. 2012 time scale [64].

The Habitats of *Peregrinella*

To date, three *Peregrinella*-bearing limestones have unequivocally been identified as ancient methane-seep deposits using a combination of petrographic, stable isotope, and biomarker analyses [19,35,37,40,42]. Appropriate material to carry out at least some of these analyses was available from a further seven localities: Bonanza Creek, Curnier, Incoronata, Musenalp, Raciborsko, Rice Valley, and Rottier. Characteristic petrographic features of seep carbonates are authigenic, early diagenetic carbonate phases, such as microcrystalline calcite (micrite), yellow calcite, and banded and botryoidal aggregates of fibrous cement [39], and the carbon isotope signature of these early diagenetic carbonate phases typically have very negative $\delta^{13}C$ signatures, significantly lower than marine bicarbonate and occasionally even lower than −50‰ [65]. A detailed description and discussion of the petrographic and stable isotope data of each locality would exceed the scope of the present paper. Therefore we provide a summary of the characteristics of the investigated sites (Table 2) and discuss their implications for reconstruction of the paleoenvironmental conditions under which *Peregrinella* lived. Representative thin section images are shown in Figure 5, and the stable isotope data are summarized in Table 3A and plotted in Figure 6.

The investigated occurrences of *Peregrinella* in this study fall within three categories:

1) Occurrences where *Peregrinella* has clearly been transported away from its original living place: Incoronata and Musenalp. Both show bedding and alignment of *Peregrinella* shells parallel to bedding (although less obvious in the case of the Musenalp). Both lack typical seep cements (Figures 5A, B), and both have $\delta^{13}C$-signatures of marine carbonate (Figure 6). No conclusions can be drawn about the original habitat of *Peregrinella* at these sites. In the case of the Incoronata locality, which overlies the mid-Valanginian drowning surface between the Maiolica pelagic limestones and the underlying coarse-grained slope debrites, *Peregrinella* has been considered as a disaster taxon that bloomed due to the environmental disruptions linked to the late Weissert Oceanic Anoxic Event [33,66].

2) *In situ* occurrences within carbonate settings with only minor ^{13}C depletion: Curnier and Rottier. The limestones of both sites show evidence for bioturbation, they lack typical seep cements, but authigenic micrites are present (Figures 5C, D). Their carbon isotope signatures (as low as −6.9 and −5.6‰, respectively, Figures 6, Table 2) are below that of marine carbonate, but clearly not low enough to rule out carbon sources other than methane. However, considering that they were deposited in an carbonate setting, a strong input of marine carbonate is obvious, which would have diluted a potentially much lower original signal [37,65]. We were not able to reproduce the extremely high $\delta^{13}C$ values of up to +20‰, as reported earlier from Rottier [18]. The accompanying mollusk fauna at Curnier and Rottier consists of taxa that are otherwise found exclusively at methane-seep deposits [30,67]. Furthermore, the presence of ^{13}C-depleted PMI and phytane in the Curnier limestone (see below) indicates that anaerobic oxidation of methane occurred in the depositional environment [65], agreeing with methane seepage. The *Peregrinella*-bearing limestones at Curnier and Rottier are therefore interpreted as ancient methane-seep deposits, probably reflecting diffuse seepage sites.

3) *In situ* occurrences in carbonate bodies with ^{13}C-depleted early diagenetic cements: Bonanza Creek, Raciborsko, and Rice Valley. Authigenic micrites, and typical seep cement such as banded and botryoidal cement are common in these limestones (Figures 5F-H, Table 2). The carbon isotope signatures of these cements are as low as −33.7 to −21.5‰ (Figure 6, Table 2) and are thus well within the range of other *Peregrinella*-bearing seep limestones [19,35,42]. The associated fauna, where present, consists largely of seep-endemic mollusks [41]. Therefore, Bonanza Creek, Raciborsko, and Rice Valley are here also identified as ancient seep deposits.

Lipid biomarker data have been reported for *Peregrinella*-bearing seep limestones from the Wilbur Springs [40], Planerskoje [37], and Zizin Valley [42] localities. For this study two new limestone samples suited for biomarker analyses were available. The hydrocarbon fraction of the Curnier limestone is typified by an unresolved complex mixture (Figure 7), reflecting a crude oil

Table 2. Summary of ecologic and environmental characteristics of *Peregrinella*-bearing localities, compiled from our own data and the literature.

Locality	Species	Max. size (mm)	Type of tectonic margin	Range of $\delta^{13}C$-values [‰]*[1]	Seep cement (%)	Mean $\delta^{18}O$-paleotemperature (°C)	References
Bonanza Creek, Alaska	*P. chisania*	30	active	−22.3 to −19.8	~20	nd	[20] and herein
Yongzhu bridge	*P. donqoensis, P. baingoinensis, P. cheboensis*	49*[2]	active	nd	nd	nd	[21]
Rice Valley, USA	*P. whitneyi*	40	active	−21.5 to −12.9	~20	12.2	[99] and herein
Wilbur Springs, USA	*P. whitneyi*	60	active	−24.3 to −19.3	10	13.3	[39] and herein
E of Lhasa, China	*P. gongboxueensis*	62.8	active	nd	nd	nd	[21]
Koniakov Castle, Czech Republic	*P. multicarinata*	26	passive	nd	nd	nd	[11]
Musenalp, Switzerland	*P. subsilvana*	56	passive	1.7 to 2.1	0	17.3	[14] and herein
Raciborsko, Poland	*P. multicarinata*	59	passive	−33.7 to −2.8	<10	nd	[13] and herein
Curnier, France	*P. multicarinata*	70	passive	−6.9 to 0.1	0	14	herein
Zizin Valley, Romania	*P. multicarinata*	85	passive	−29.7 to −20.4	5	12.2	[42]
Incoronata, Italy	*P. garganica*	85	passive	−3.1 to −1.2	0	nd	[32] and herein
Chatillon, France	*P. multicarinata*	85	passive	nd	nd	15.1	herein
Rottier, France	*P. multicarinata*	88	passive	−5.6 to 2.2	0	13.8	[29] and herein
Planerskoje, Crimea	*P. multicarinata*	90	passive	−13.6 to 2.9	<5	11.7	[35]
Koniakov, Czech Republic	*P. silesica*	90	passive	nd	nd	nd	[11]
Kuban, Russia	*P. pinguis*	102	passive	nd	nd	nd	[102]

nd = no data,
*[1]: only the values of carbonate mineral phases are given here, not those of *Peregrinella* shells;
*[2]: size of largest species.
doi:10.1371/journal.pone.0109260.t002

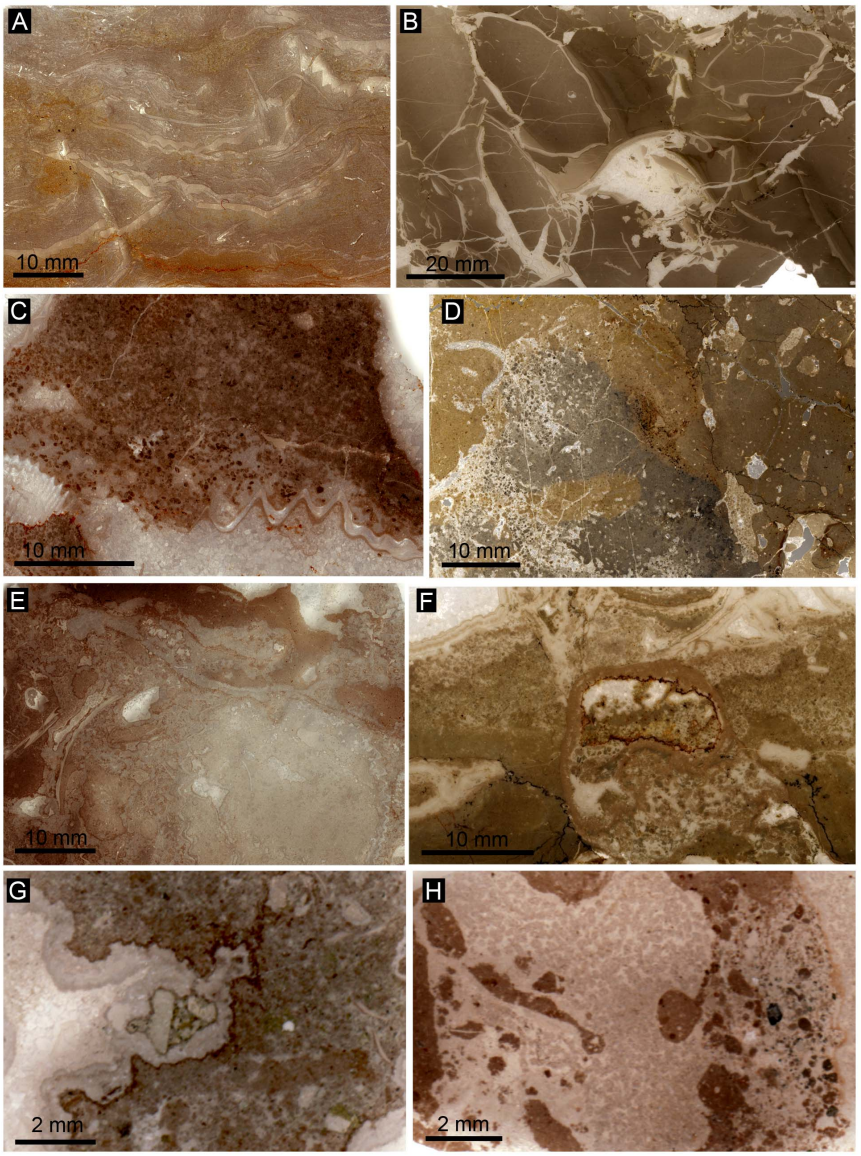

Figure 5. Petrography of *Peregrinella* limestones. Images are ordered by an increasing proportion of seep cements (light colored), compared to microcrystalline carbonate (micrite; dark colored). A: Incoronata (GZG.INV.82754); B: Musenalp (GZG.INV.82734); C: Rottier (FSL 425077); D: Curnier (GZG.INV.82728); E: Rice Valley (GZG.INV.82748); F: Wilbur Springs (GZG.INV.82753); G: Bonanza Creek (USNM 603602), H: Raciborsko (ZPAL Bp.III).
doi:10.1371/journal.pone.0109260.g005

pattern and indicating pronounced biodegradation. The timing of possible oil ingress and biodegradation cannot be constrained with certainty. Thus, the possibility of syndepositional oil seepage cannot be ruled out. Although the observed compound pattern has obviously been affected by biodegradation and thermal maturity, two compounds and their carbon isotopic compositions point to syndepositional methane seepage, having fueled the anaerobic oxidation of methane involving methanotrophic archaea. Irregular, ^{13}C-depleted pentamethylicosane (PMI) is a stable and particularly long-lasting biomarker of methanotrophic archaea [65,68]. Its δ^{13}C value of −48‰ is much higher than values of PMI typically observed at methane seeps; yet, it is also much lower than the values of the regular isoprenoid pristane in the same sample, the precursors of which are produced by phototrophs [69]. Most likely, the relatively high δ^{13}C value of PMI is due to masking of its pristine isotopic signature caused by the unresolved complex mixture made up of compounds with higher ^{13}C content, on average, than PMI. Hence, it is difficult to determine whether the observed intermediate value of PMI represents a pure methanotrophic or mixed source (methanotrophic and methanogenic archaea) signal. Moreover, the isotopic composition of the regular isoprenoid phytane (−44‰) is much lower than that of pristane (−35‰), revealing that phytane did not exclusively derive from phototrophic organisms. The greater ^{13}C-depletion of phytane is best explained by input from methanotrophic archaea (archaeal diethers), in addition to input from phototrophic organisms (chlorophyll), resulting in a carbon isotopic composition that falls between the compositions commonly observed for lipids of methanotrophs and phototrophs. To sum up, in combination with the lowest $\delta^{13}C_{carbonate}$ values of −6.9‰ found for the Curnier limestone, the observed lipid patterns are best explained by anaerobic oxidation of methane at a seafloor seep. The seepage fluids also may have included crude oil or, alternatively, oil may have intruded the limestone at a later stage. Unlike the Curnier

Table 3. Summary of the stable carbon and oxygen isotope data.

A - Limestone samples			**B - *Peregrinella* shells**			
Sample	**$\delta^{13}C$(PDB) [‰]**	**$\delta^{18}O$(PDB) [‰]**	**Sample**	**$\delta^{13}C$ (PDB) [‰]**	**$\delta^{18}O$ (PDB) [‰]**	**Paleotemperature [°C]**
Bonanza Creek, micrite	−19.8	−15.6	Châtillon, FSL 425076	0.0	−0.5	**14**
Bonanza Creek, micrite	−20.3	−17.6	Châtillon, FSL 425076	−0.1	−0.9	**16**
Bonanza Creek, rim cement	−20.0	−9.8	Châtillon, FSL 425076	0.1	−0.6	**14**
Bonanza Creek, rim cement	−22.3	−7.9	Châtillon, FSL 425076	0.2	−1.0	**16**
Bonanza Creek, rim cement	−21.5	−10.3	Curnier, shell 1, GZG.INV.82725	0.5	−0.3	**13**
Curnier, micrite, GZG.INV.82728	−4.3	−1.3	Curnier, shell 1, GZG.INV.82725	0.7	−0.2	**13**
Curnier, micrite, GZG.INV.82728	−3.9	−1.0	Curnier, shell 2, GZG.INV.82726	−0.3	−1.6	**18**
Curnier, micrite, GZG.INV.82728	−2.8	−0.7	Curnier, shell 2, GZG.INV.82726	−0.3	−1.1	**17**
Curnier, micrite, GZG.INV.82728	−2.0	−1.6	Curnier, shell 3, GZG.INV.82727	0.3	0.1	**12**
Curnier, micrite, GZG.INV.82728	−1.3	−0.5	Curnier, shell 3, GZG.INV.82727	0.9	0.2	**11**
Curnier, micrite, GZG.INV.82728	−6.9	0.0	Musenalp, shell 1, GZG.INV.82735	0.8	−1.3	**17**
Curnier, micrite, GZG.INV.82728	−5.2	−0.1	Musenalp, shell 2, GZG.INV.82736	1.1	−1.7	**19**
Curnier, micrite, GZG.INV.82728	−2.9	−2.5	Musenalp, shell 3, GZG.INV.82730	0.4	−1.1	**16**
Curnier, micrite, GZG.INV.82728	−1.8	−0.9	Musenalp, shell 4, GZG.INV.82731	1.1	−0.8	**15**
Curnier, micrite, GZG.INV.82728	−2.0	0.3	Musenalp, shell 5, GZG.INV.82732	1.0	−1.3	**17**
Curnier, micrite, GZG.INV.82728	−1.9	−0.1	Musenalp, shell 5, GZG.INV.82732	0.9	−1.7	**19**
Curnier, micrite, GZG.INV.82728	−4.1	0.2	Planerskoje, shell 1, GZG.INV.82739	−1.4	0.1	**11**
Curnier, micrite, GZG.INV.82728	−2.3	−0.3	Planerskoje, shell 2, GZG.INV.82740	−0.1	0.1	**12**
Curnier, micrite, GZG.INV.82728	−2.1	−0.4	Planerskoje, shell 3, GZG.INV.82741	−0.2	0.0	**12**
Curnier, rim micrite, GZG.INV.82728	0.1	0.4	Planerskoje, shell 4, GZG.INV.82742	−0.8	0.1	**12**
Curnier, rim micrite, GZG.INV.82728	−1.2	0.2	Planerskoje, shell 5, GZG.INV.82743	−0.8	0.0	**12**
Curnier, rim micrite, GZG.INV.82728	−0.8	0.1	Planerskoje, shell 6, GZG.INV.82744	−2.5	0.0	**12**
Incoronata, Italy, GZG.INV.82754	−3.2	−3.3	Rice Valley, GZG.INV.82748	−1.7	−0.5	**14**
Incoronata, Italy, GZG.INV.82754	−1.8	−2.9	Rice Valley, GZG.INV.82749	−3.0	−0.3	**13**
Incoronata, Italy, GZG.INV.82754	−1.3	−2.4	Rice Valley, GZG.INV.82750	−0.6	−0.1	**12.**
Musenalp, micrite, GZG.INV.82733	2.1	−4.9	Rice Valley, GZG.INV.82751	0.8	0.2	**11**
Musenalp, micrite, GZG.INV.82733	1.9	−5.1	Rice Valley, GZG.INV.82752	−2.8	0.4	**10**
Musenalp, micrite, GZG.INV.82733	1.7	−0.8	Rottier, FSL 425077	0.2	−0.2	**13**
Musenalp, micrite, GZG.INV.82733	2.1	−0.2	Rottier, FSL 425077	0.0	−0.3	**13**
Musenalp, micrite, GZG.INV.82733	2.0	−0.4	Rottier, FSL 425078	0.3	−1.3	**18**
Musenalp, micrite, GZG.INV.82733	2.0	−3.9	Rottier, FSL 425078	−2.6	−1.2	**17**
Musenalp, micrite, GZG.INV.82733	2.1	−3.6	Rottier, FSL 425079	−0.1	0.1	**12**
Musenalp, micrite, GZG.INV.82733	1.9	−0.7	Rottier, FSL 425079	0.0	0.2	**11**
Musenalp, micrite, GZG.INV.82733	2.0	−0.3	Wilbur Springs, GZG.INV.82753	−1.1	−0.4	**13**
Musenalp, sparitic rim in shell, GZG.INV.82734	1.9	−0.6	Wilbur Springs, USNM 603596	−1.4	−0.4	**14**
Musenalp, sparitic rim in shell, GZG.INV.82734	1.9	−0.3	Wilbur Springs, USNM 603597	−0.6	−0.2	**13**
Musenalp, sparitic rim in shell, GZG.INV.82734	2.0	−1.0	Wilbur Springs, USNM 603598	−2.5	−1.0	**16**
Musenalp, sparitic rim in shell, GZG.INV.82734	2.1	−0.7	Wilbur Springs, USNM 603599	−0.4	0.2	**11**
Raciborsko, micrite, ZPAL Bp.III	−33.7	0.1	Zizin Valley, LPB III br 364	0.1	0.1	**12**
Raciborsko, peloidal micrite, ZPAL Bp.III	−2.8	−9.1	Zizin Valley, LPB III br 372	0.0	−0.3	**13**
Raciborsko, micrite, ZPAL Bp.III	−24.8	−1.1	Zizin Valley, LPB III br 381	0.3	0.1	**12**
Raciborsko, peloidal micrite, ZPAL Bp.III	−3.4	−8.8	Zizin Valley, LPB III br 381	0.3	0.1	**11**
Rice Valley*	−21.5	0.6	Zizin Valley, LPB III br 389	0.4	−0.4	**13**
Rice Valley*	−12.9	3.2				
Rice Valley*	−20.7	1.1				
Rice Valley*	−17.6	1.3				
Rottier, micrite, FSL 425077	2.2	−1.5				

Table 3. Cont.

A - Limestone samples			B - *Peregrinella* shells			
Sample	**$\delta^{13}C$(PDB) [‰]**	**$\delta^{18}O$(PDB) [‰]**	**Sample**	**$\delta^{13}C$ (PDB) [‰]**	**$\delta^{18}O$ (PDB) [‰]**	**Paleotemperature [°C]**
Rottier, micrite, FSL 425077	−5.3	−2.8				
Rottier, micrite, FSL 425077	−5.4	−2.5				
Rottier, micrite, FSL 425077	−5.6	−2.9				
Rottier, micrite, FSL 425077	−5.4	−1.6				
Rottier, micrite, FSL 425077	−4.9	−1.4				
Rottier, micrite, FSL 425077	−4.5	−1.0				
Rottier, rim micrite, FSL 425077	−4.2	−2.8				
Rottier, rim micrite, FSL 425077	−4.4	−2.6				

*Data from [99].
doi:10.1371/journal.pone.0109260.t003

limestone, no biomarker evidence for seepage was found for the Musenalp limestone, agreeing with its marine $\delta^{13}C_{carbonate}$ values (Figure 6). No irregular isoprenoids were detected in the Musenalp sample, and the regular isoprenoids pristane and phytane as well as *n*-alkanes yielded $\delta^{13}C$ values (−31 to −30‰) that are typical for lipids resulting from marine primary production in the photic zone [70].

Impact of *Peregrinella* on Other Seep Inhabitants

The sheer abundance of *Peregrinella* at the localities it colonized (Figure 1) has led to suggestions that it had a negative impact on at least some of the co-occurring taxa, in particular infaunal and semi-infaunal bivalves [19,35], but these suggestions were based only on observations for individual *Peregrinella* occurrences. We therefore attempted to address this question in a more comparative way. The mollusks in methane-seep communities of the late Mesozoic show an overall similarity in faunal composition, although with a notable turnover during the mid-Cretaceous, and are often dominated by the modiomorphid bivalve *Caspiconcha*, several seep-restricted lucinid bivalves, and the gastropod *Hokkaidoconcha* [8,30,71–75]. Therefore, our comparisons of specimen size and diversity of the seep mollusk fauna in the presence or absence of *Peregrinella* focused on two time intervals: first the late Jurassic through late Cretaceous (henceforth referred to as the 'late Mesozoic'), to assess possible impacts of *Peregrinella* on the late Mesozoic seep fauna in general, and second only the time interval spanning the stratigraphic range of *Peregrinella* (henceforth referred to as the '*Peregrinella* interval'). The faunal data for these analyses and their sources are summarized in Table 4; included are only sites where we had some confidence that the fauna had been adequately sampled, i.e., reports of *Peregrinella* from collections with unknown sampling strategies (such as Bonanza Creek or Châtillon-en-Dois reported here) are not included.

We performed a set of tests with each of the three infaunal chemosymbiotic bivalve families Solemyidae, Thyasiridae and Lucinidae. First, for the late Mesozoic we tested whether they were more commonly (1) present, and (2) larger, at seep sites outside the *Peregrinella* interval than at seep sites during the *Peregrinella* interval. Second, for the *Peregrinella* interval we tested whether they were (1) more frequently absent from, and (2) smaller at sites with *Peregrinella* than at sites without *Peregrinella*. For the size tests, only the largest record was used when more than one species of a family was present at a locality.

During the late Mesozoic, all three bivalve families were neither more common nor larger at seep sites outside the *Peregrinella* interval than during the *Peregrinella* interval (Figure 8). However,

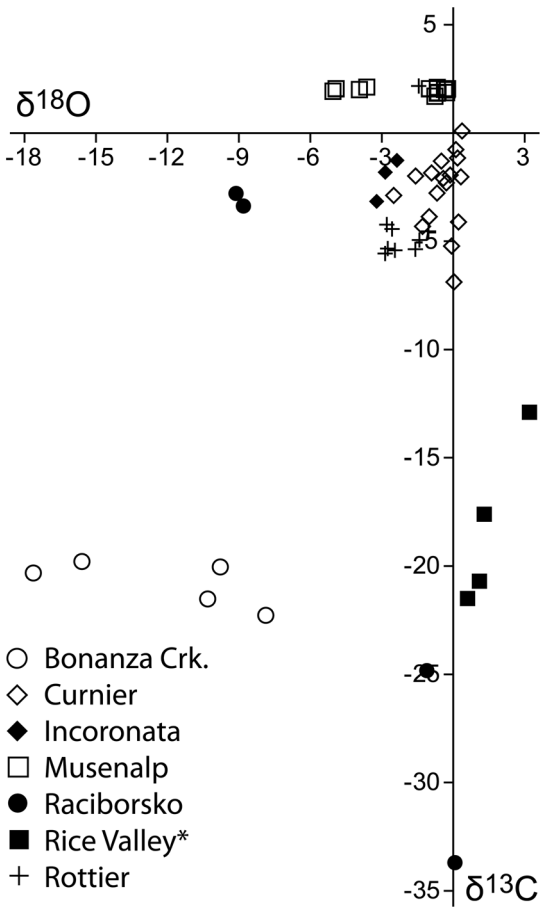

Figure 6. Carbon and oxygen isotope values of *Peregrinella*-bearing limestones. All values are reported relative to the PDB standard. * Data from [99].
doi:10.1371/journal.pone.0109260.g006

in the case of the thyasirids these comparisons are problematic: they were reported from shallow-water seeps from the Berriasian on Svalbard [76], are entirely absent from seeps during the remainder of the lower half of the Early Cretaceous, and re-appear in the Albian of Japan and New Zealand [77,78]. An alternative explanation to a potential impact of *Peregrinella* is that thyasirids did not colonize deep-water seeps until Albian time.

When only the *Peregrinella* interval was considered, lucinids were neither more frequently absent from, nor smaller at sites with *Peregrinella* than at sites without *Peregrinella*. In a rigorous statistical sense this is also true for the solemyids (Fisher's exact test, $p = 0.23$), although it is remarkable that solemyids occur at all non-*Peregrinella* sites but only at a single site with *Peregrinella* (Table 4). In summary, contrary to previous suggestions, we found little empirical evidence that *Peregrinella* had a negative impact on the presence or size of infaunal bivalves at seeps. However, the observation from the seep deposit at Wilbur Springs that *Peregrinella* is more abundant than the co-occurring modiomorphid bivalves [19] (Figure 1) also applies to the infaunal chemosymbiotic bivalves.

At localities where *Peregrinella* occurs, it is always more abundant than any other taxon. Therefore, we were interested in whether the presence of *Peregrinella* affected species diversity at the sites it colonized. For the *Peregrinella* interval we tested whether seep sites with fewer than 10 associated species (i.e., excluding *Peregrinella*) are more common among the *Peregrinella*-bearing deposits than seep sites with more than 10 associated species. Sites without associated species were excluded. This analysis showed no significant difference (Fisher's exact test, $p = 0.56$, Table 5). At its various occurrences, *Peregrinella* coexisted with virtually all coeval seep mollusks, as well as occasional tube worms and sponges. Neither the origin nor the extinction of *Peregrinella* coincides with the origin or extinction of any coeval seep-inhabiting mollusk (Figure 9).

Environmental Impacts on *Peregrinella*

Peregrinella reached significantly greater maximum sizes at passive continental margins than at active margins (Mann-Whitney *U* test, $p = 0.04$; Table 2). Assuming that environmental disturbances such as turbidites are more common at active

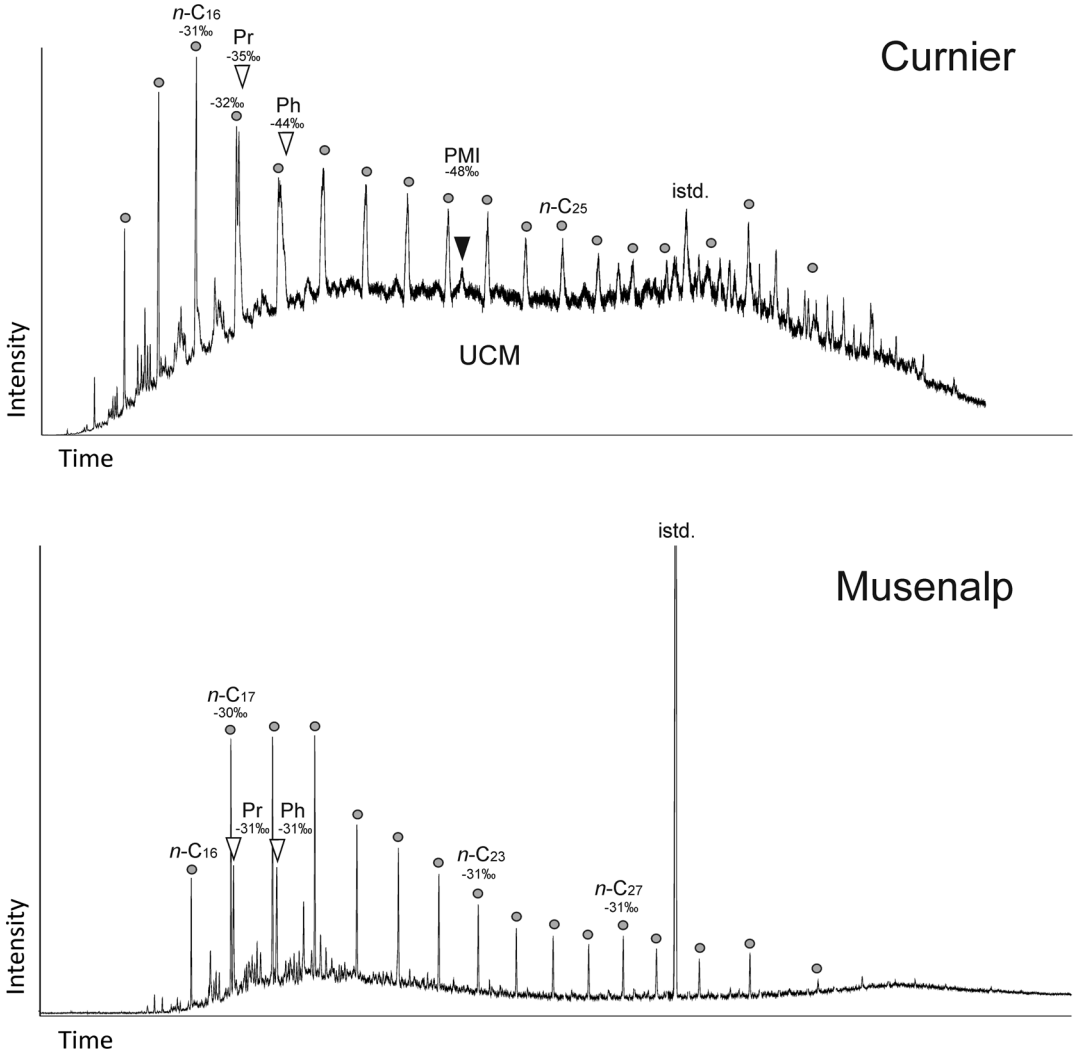

Figure 7. Hydrocarbon fractions (total ion currents) of the Curnier and Musenalp limestones with *Peregrinella*. Circles: *n*-alkanes; white triangles: regular isoprenoids; black triangles: irregular isoprenoids; Pr: pristane; Ph: phytane; PMI: pentamethylicosane; istd.: internal standard; UCM: unresolved complex mixture; compound-specific $\delta^{13}C$ values are indicated in per mil relative to the Peedee belemnite standard.
doi:10.1371/journal.pone.0109260.g007

Table 4. *Peregrinella* and chemosymbiotic bivalves at Cretaceous seep deposits.

Locality (age)	*Peregrinella*	Solemyidae, size (mm)	Thyasiridae, size (mm)	Lucinidae, size (mm)	References
Beauvoisin (Oxfordian)	**a**			*Beauvoisina carinata*, 200	[103]
Gateway Pass (Tithonian)	**a**			lucinid, 50	[104]
NW Berryessa (Tithonian)	**a**			*Tehamatea ovalis*	[41]
Paskenta (Tithonian)	**a**	*Acharax stantoni*, 58		*Tehamatea ovalis*, 60	[41,105]
				Tehamatea colusaensis, 95	
Stony Creek (Tithonian)	**a**	*Acharax stantoni*		*Tehamatea colusaensis*	[41]
				Tehamatea ovalis	
*** Sassenfjorden (Berriasian)**	**a**	solemyid, 77	thyasirid, 50	lucinid, 94	[76]
*** Planerskoje (Berriasian)**	**p**			*Tehamatea vocontiana*, 70	[30,35]
*** Musenalp (Berriasian)**	**p**				[14] and herein
*** Bear Creek (Valanginian)**	**a**	*Acharax stantoni*, 60		*Tehamatea ovalis*, 25	[30,101]
*** Little Indian Valley (Valanginian)**	**a**	*Solemya* sp.			[41]
*** Rocky Creek (Valanginian)**	**a**	*Acharax stantoni*, 56		*Tehamatea colusaensis*, 145	[30]
*** Raciborsko (Hauterivian)**	**p**				[13] and herein
*** Koniakov (Hauterivian)**	**p**			*Lucina* sp., 22	[11,106]
*** Koniakover Schloss (Hauterivian)**	**p**			*Lucina valentula*, 13	[11,106]
				Lucina obliqua, 11	
				lucinid sp. ind., 70	
*** Curnier (Hauterivian)**	**p**			*Tehamatea vocontiana*, 50	herein
*** Rottier (Hauterivian)**	**p**			*Tehamatea vocontiana*, 200	[30]
*** Wilbur Springs (Hauterivian)**	**p**	*Acharax stantoni*, 70		*Tehamatea colusaensis*, 77	[30,105]
Baska (Barremian)	**a**			lucinid indet., 30	[106]
Eagle Creek (Barremian)	**a**	*Acharax stantoni*, 47		*Tehamatea ovalis*	[101]
Kuhnpasset Beds (Barremian)	**a**	*Solemya* sp., 50		*Amanocina kuhnpassetensis*, 129	[107]
Awanui I (Albian)	**a**			*Cubathea awanuiensis*, 27	[30,78]
				Amanocina raukumara, 33	
Awanui II (Albian)	**a**			*Cubathea awanuiensis*, 50	[30,78]
CFCC (Albian)	**a**	*Acharax stantoni*, 35		*Lucina* sp., 22	[30]
Ispaster (Albian)	**a**			*Tehamatea agirrezabalai*, 135	[30,108]
Ponbetsu (Albian)	**a**	*Acharax mikasaensis*, 55	*Thyasira tanabei*, 11.7	"*Nipponothracia*" *ponbetsensis*, 120	[77]
Awanui GS 688 (Cenomanian)	**a**		thyasirid, 6	*Amanocina raukumara*, 80	[30,78]
				Cubathea awanuiensis, 48	
				Ezolucina ? sp. "ridge", 37	
Obira-cho (Cenomanian)	**a**	solemyid indet.	*Thyasira tanabei*, 10.4	lucinid indet., 43	[77]
				Miltha sp.	
				Amanocina yezoensis, 100	
Omagari lens (Campanian)	**a**		*Thyasira tanabei*, 50	lucinid *ponbetsensis*, 60	[77]
				Tehamatea sp.?, 50	
Romero Creek (Campanian)	**a**	*Solemya* sp.	*Thyasira cretacea*		[41]
Sada Limestone (Campanian)	**a**	solemyid, 70	*Thyasira hataii*, 80	*Myrtea*? sp., 35	[30,109]
				lucinid, 71	
Waipiro I (Campanian)	**a**			*Ezolucina* sp., 120	[30,78]
Waipiro III (Campanian)	**a**	solemyid, 20	thyasirid, 10	lucinid, 30	[30,78]
Yasukawa (Campanian)	**a**	*Acharax cretacea*, 60	*Thyasira tanabei*, 10.4	*Miltha* sp., 18	[110]
				Myrtea sp., 10	

* = sites of the *Peregrinella* interval, a = absent, p = present.

doi:10.1371/journal.pone.0109260.t004

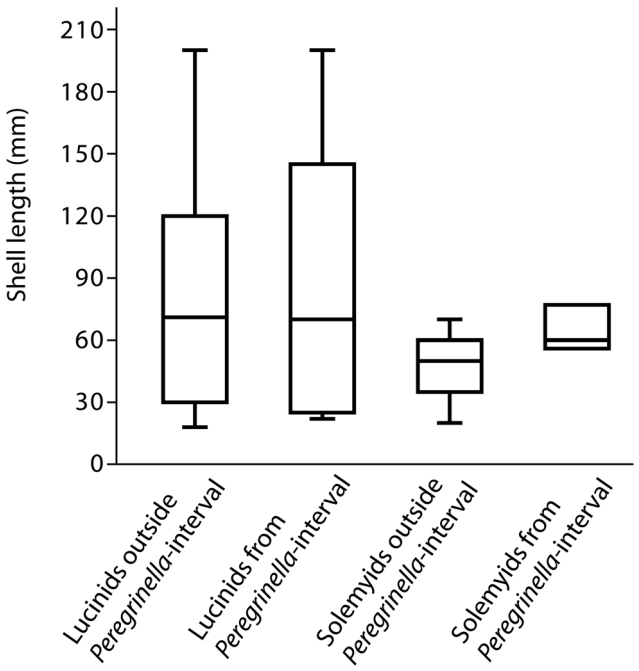

Figure 8. Shell sizes of chemosymbiotic bivalves at late Mesozoic methane seeps.
doi:10.1371/journal.pone.0109260.g008

margins than in deep shelf settings at passive margins, it may be inferred that *Peregrinella* was sensitive toward such environmental disturbances.

The intensity of seep fluid flow plays a major role in structuring seep communities today because some taxa prefer sites with focused, advective fluid flow while others prefer sites of slow, diffusive seepage [79]. The apparent restriction of *Peregrinella* to seeps suggest that it benefited, in as-yet unknown ways, from the seeping fluids and the reduced compounds in them. Most likely, *Peregrinella* benefited from chemotrophic bacteria using methane and/or sulfide, but whether *Peregrinella* was filter-feeding on free-living bacterioplankton, for example like modern vent and seep-inhabiting barnacles [80], or had a symbiotic relationship with such bacteria, remains unknown and cannot be resolved with the data presented here. We were interested whether *Peregrinella* had a preference for a certain paleo-seep fluid intensity and compared the maximum size of *Peregrinella* to two proxies for seepage intensity: (i) the carbon isotope signature of the enclosing limestone, and (ii) the abundance of the typical seep cements such as banded or botryoidal cement, quantified based on thin section observations; the localities with uncertain original habitat type, Incoronata and Musenalp, were not used in this comparison. There is no correlation between the maximum size of *Peregrinella* and the carbon isotope signature of the enclosing limestone, but we found a significant negative correlation between the maximum size of *Peregrinella* and the abundance of seep cements (i.e. fibrous, banded and botryoidal cement rather than micrite): *Peregrinella* is on average larger at sites with fewer seep cements ($p<0.003$, Table 2), suggesting that it was better adapted to diffusive rather than advective seepage [37].

Paleo-temperatures calculated from $\delta^{18}O$ values of *Peregrinella* shells indicate that these specimens lived at temperatures ranging from 10 to 19°C (Tables 2, 3B). At some localities different shells showed a remarkably uniform range of values (i.e., Planerskoje: 11 to 12°C) while at other localities different shells showed a wide scatter of values (i.e., Rottier: 11 to 18°C; Curnier: 11 to 18°C). The data are summarized in Figure 10. These absolute values should be treated cautiously because some rhynchonellid brachiopods exert vital effects when incorporating oxygen isotopes into their shells [46]. But because we investigated only specimens of a single genus, we infer that all investigated specimens lived within a temperature range spanning about 9°C from the coldest to the warmest. Does this reflect the preferred temperature range of the genus *Peregrinella* in general? Unfortunately, the available material from the northernmost occurrence, the Alaskan Bonanza Creek site, was too sparse for oxygen isotope analyses. Therefore *Peregrinella* might have lived also at lower temperatures than inferred here and thus might have had a broader temperature range than the 9°C estimated from the available specimens.

Brachiopod Geologic Ranges

The 9 m.y. long geologic range of *Peregrinella* appears short when compared to genera of seep-inhabiting mollusks, including chemosymbiotic bivalves, which may reach geologic ranges of 50 m.y. or more [4,30]. But how does this compare to the geologic ranges of other brachiopod genera? Virtually all brachiopod genera that dominated vent and seep deposits in the geologic past belong to a single rhynchonellid superfamily, the Dimerelloidea [22,24–27,81] and their geologic ranges seem to never exceed 10 m.y. in duration (see fig. 9.6 in [23]). To investigate how the geologic ranges of *Peregrinella* and other dimerelloids compare to those of rhynchonellid brachiopod genera in general, we summarized the geologic ranges of genera of the Rhynchonellida listed in Sepkoski's compendium [82], using the following criteria: only taxa with their first appearances (FAs) and last appearances (LAs) given at least to series level were included. Only taxa having their FAs in Devonian through Cretaceous were included. Subgenera and genera with "?" were excluded. Taxa with questionable FAs or LAs, as indicated by a "?" were excluded. Stratigraphic subdivisions such as lower, middle, and upper were ignored. Taxa with FAs or LAs in the Leonardian (Permian) were excluded because this stage could not be correlated with the Gradstein et al. 2012 time scale [64]. The geologic ranges of the remaining 483 genera were calculated as follows: numerical age of base of FA minus numerical age of end of LA. This resulted in a median geologic range of 12.7 m.y., and 25 and 75 percentiles of 6.6 and 17.3 m.y., respectively. Thus the 9 m.y. range of *Peregrinella* and the geologic ranges of dimerelloid genera in general, are somewhat shorter than the median, but certainly not abnormal for rhynchonellid brachiopods. In this respect, dimerelloids differ from mollusk genera at seeps which are, on average, longer-lived than marine mollusks in general [4]. These observations fit with two macroevolutionary patterns among brachiopods and mollusks. First, on low taxonomic levels (e.g., genus, species) brachiopods show higher origination and extinction rates than mollusks [83,84], as seen here also among their seep-inhabiting members. Second, on the family/superfamily level brachiopods appear to persist longer in deep-water environments than gastropods do [85], consistent with the long persistence of the Dimerelloidea in the vent/seep environment.

Discussion

The oldest occurrences of *Peregrinella* are the Musenalp site in Switzerland and the Planerskoje site in the eastern Crimean peninsula; both are of late Berriasian age. The genus thus apparently originated in the Tethys Ocean [21], in contrast to a previous hypothesis of an origin in California and subsequent dispersal to Europe [13,45]. In the Valanginian *Peregrinella* had

Table 5. Numbers of species at seep deposits from the *Peregrinella* interval; a = absent, p = present.

Locality	# associated species	*Peregrinella*	Reference
Musenalp, Switzerland	1	p	[14]
Curnier, France	2	p	herein
Rottier, France	2	p	[29] and herein
East Berryessa, USA	3	a	[41]
Foley Canyon, USA	3	p	[41]
Gravelly Flat, USA	3	p	[41]
Rice Valley, USA	4	p	[41]
West Berryessa, USA	4	a	[41]
Little Indian Valley, USA	5	a	[41]
Koniakov, Czech Republic	5	p	[11,106]
Planerskoje, Crimean peninsula	7	p	[35]
Wilbur Springs, USA	10	p	[41,71]
Rocky Creek, USA	13	a	[41,71,101]
Koniakov Castle, Czech Republic	17	p	[11,106]
Bear Creek, USA	18	a	[41,71,101]

doi:10.1371/journal.pone.0109260.t005

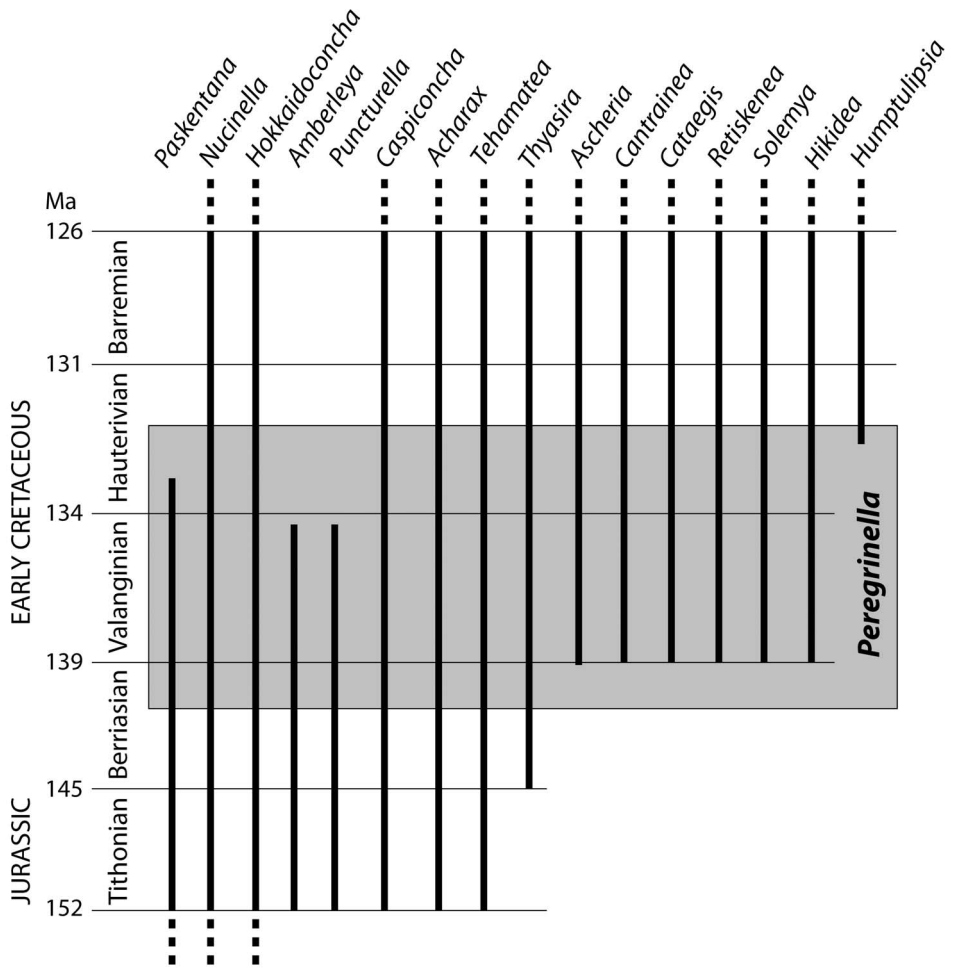

Figure 9. Geologic ranges of seep-inhabiting mollusk genera and *Peregrinella* during the Late Jurassic – Early Cretaceous. Data from [8,25,30,41,61,67,74,100,101]; absolute ages from [64].
doi:10.1371/journal.pone.0109260.g009

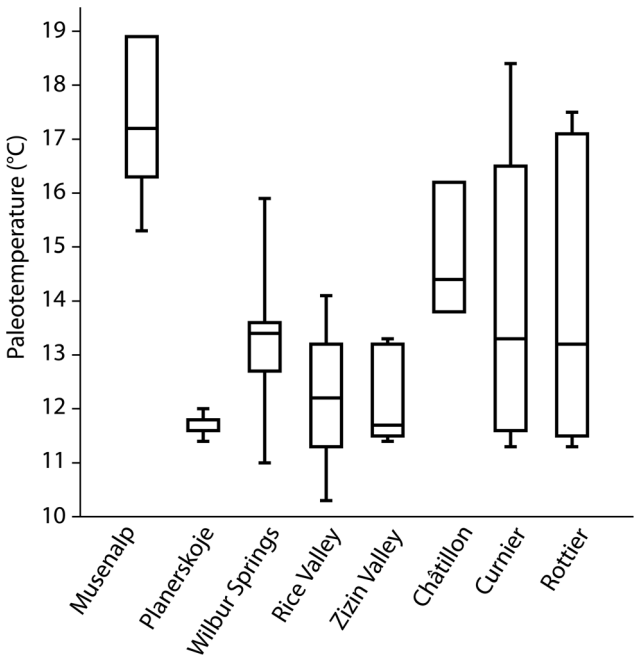

Figure 10. Paleotemperatures derived from $\delta^{18}O$ values of *Peregrinella* shells. Localities ordered from oldest (left) to youngest (right).
doi:10.1371/journal.pone.0109260.g010

spread eastward as far as Tibet [21] and by Hauterivian time it had spread to California and Alaska. Whether this spread to the American West coast was eastward or westward from the Tethys remains unclear. The present understanding of Early Cretaceous ocean currents [86] makes a westward spread possible, although an eastward spread along the active continental margins around the North Pacific Ocean also seems plausible [87]. The youngest occurrences are those from southern France and Alaska, and are of late early Hauterivian age.

The timing of the appearance and disappearance of *Peregrinella* is puzzling, because neither does it coincide with the appearance and disappearance of any other seep-inhabiting taxon, nor with any of the major oceanic disturbances such as oceanic anoxic events (OAEs). Its extinction at the end of the early Hauterivian roughly coincides with the 'Faraoni event', a presumed, short-lived anoxic event in the late Hauterivian [88], but this event was apparently restricted to the Tethyan Realm and does not explain the disappearance of *Peregrinella* from California and Alaska.

The implied concurrent demise of *Peregrinella* and the large, seep-inhabiting bivalve *Caspiconcha* at Cretaceous seeps in figure 15 of [74] is not supported by our Sr-isotope stratigraphy results and by the finding of a mid-Cenomanian *Caspiconcha*-dominated seep deposit in New Zealand [78]. There are about 36 m.y. between the extinction of *Peregrinella* at the end of the early Hauterivian and the last *Caspiconcha*-dominated seep deposit.

The apparent preference of *Peregrinella* for diffusive seepage rather than for focused, advective fluid flow is surprising considering that taxa dominating modern vents and seeps prefer strong fluid flow and resulting high hydrogen sulfide concentrations [79,89,90]. A potential implication of this pattern is that the link of *Peregrinella* to seeps is related to methane rather than to hydrogen sulfide. Because hydrogen sulfide is quickly oxidized in the presence of oxygen, it only reaches the seafloor when fluid flow is strongly advective. When fluid flow is slow and diffusive, hydrogen sulfide is oxidized before it reaches the sediment-water interface, as shown by modeling approaches and *in situ* measurements [91,92]. Methane, on the other hand, is only oxidized biologically in marine environments and therefore has a greater chance to reach the sediment-water interface under diffusive flow conditions than hydrogen sulfide. In case of the Planerskoje and Zizin Valley seep deposits, the presence of molecular fossils of aerobic methane-oxidizing bacteria [37,42] reveals that at least some of the seeping methane was not oxidized in the zone of anaerobic oxidation of methane but entered the oxic zone. Based on the low preservation potential of lipids of endosymbiotic bacteria, such a source can be ruled out for the observed molecular fossils, but their presence reveals that oxygen-dependent consumption of methane indeed occurred at the ancient seep sites [93]. Thus, assuming that *Peregrinella* relied – in as-yet unknown ways – on chemotrophic bacteria, then its apparent preference for diffusive seepage may suggest a more prominent role of methane-oxidizing bacteria, rather than sulfide-oxidizing bacteria, in the diet of *Peregrinella*.

We infer the preference of *Peregrinella* for diffuse seepage from the larger average sizes of *Peregrinella* at sites with fewer seep cements. This may have implications for other seep-inhabiting dimerelloids from different geologic ages. In contrast to *Peregrinella*, certain dimerelloid genera including the Devonian *Dzieduszyckia* [26] and the Jurassic *Sulcirostra* [27], occur at sites where the proportion of seep cements of the limestone exceeds that seen in any *Peregrinella* site by a great margin, and may even constitute the majority of the limestone. These brachiopods potentially lived at seep sites with strong, advective fluid flow. The early Jurassic dimerelloid *Anarhynchia* cf. *gabbi* is common at a hydrothermal vent deposit [94] where sulfide most likely was the dominant reduced chemical compound. Therefore, it seems possible that the different dimerelloids developed various strategies for living at vent and seep environments. However, most of these genera have been documented from one or two seep deposits only, making a direct comparison with the trend seen in *Peregrinella* impossible.

Conclusions

All *in situ* occurrences of *Peregrinella* investigated here were confirmed as ancient seep deposits. This supports the view that *Peregrinella* lived exclusively at seeps [19] and calls for further investigations to determine whether other dimerelloid genera that have been reported from seep or hydrothermal-vent deposits (i.e., *Anarhynchia*, *Cooperrhynchia*, *Dzieduszyckia*, *Halorella*, *Ibergirhynchia*, *Sulcirostra*) were also restricted to this type of habitat, or had broader ecologic plasticity [26].

While the question whether *Peregrinella* was chemosymbiotic or not remains unresolved, the comparative approach used here provides new insights into the paleoecology of this enigmatic brachiopod, notably the apparent preference for living at diffusive rather than advective seepage sites. Expanding this line of work to other seep-inhabiting dimerelloids could show whether this preference is shared by dimerelloids in general or whether different dimerelloid genera had adapted to vents and seeps in different ways.

Compared to other seep-inhabiting groups, especially the well-studied mollusks, *Peregrinella* has two remarkable traits: first, its quite short geologic range of only 9 m.y., and second, its extremely gregarious mode of occurrence. However, from a rhynchonellid brachiopod's perspective, these traits may not be unusual: *Peregrinella*'s stratigraphic range is not very different from the average rhynchonellid's range, and given a suitable habitat,

rhynchonellid brachiopods tend to be gregarious [95–97]. Thus while seep mollusks clearly differ from other marine mollusks in their geologic longevity, this seems not to be the case for *Peregrinella* and perhaps also for other seep-inhabiting dimerelloids back to the Devonian.

Acknowledgments

We thank Chuck Fisher (Penn State University) for providing shells from Recent seeps for comparison, Tina Kollaske (BGR Berlin) for the loan of a putative *Peregrinella* specimen from northeastern Germany, Abel Prieur and Emmanuel Robert (Lyon) for arranging the loan of specimens from southern France, Amanda Millhouse (Washington, DC) for arranging the loan of specimens from the USNM collection, Andreas Pack (Göttingen) for stable C and O isotope analyses, Axel Hackmann (Göttingen) for thin section preparation, Dorothea Hause-Reitner (Göttingen) for assistance with the SEM, Birgit Wild and Andreas Richter (Vienna) for aid measuring compound-specific stable carbon isotopes, Beatrix Bethke (Vienna) for biomarker sample extractions, John M. McArthur (London) for providing the LOWESS 5.0 look-up table, Przemysław Gedl (ING PAN, Cracow) for discussion of Carpathian stratigraphy, and two anonymous reviewers for their insightful comments that helped to improve this manuscript.

Author Contributions

Conceived and designed the experiments: SK. Performed the experiments: SK JG DB JP. Analyzed the data: SK JG DB JP. Wrote the paper: SK JG DB JP. Conducted field work and/or contributed specimens: SK LGB KAC CG RG AK IL MRS.

References

1. Corliss JB, Dymond J, Gordon LI, Edmond JM, Von Herzen RP, et al. (1979) Submarine thermal springs on the Galápagos Rift. Science 203: 1073–1083.
2. Paull CK, Hecker B, Commeau R, Freeman-Lynde RP, Neumann C, et al. (1984) Biological communities at the Florida Escarpment resemble hydrothermal vent taxa. Science 226: 965–967.
3. Campbell KA (2006) Hydrocarbon seep and hydrothermal vent paleoenvironments and paleontology: Past developments and future research directions. Palaeogeogr Palaeoclimatol Palaeoecol 232: 362–407.
4. Kiel S, Little CTS (2006) Cold seep mollusks are older than the general marine mollusk fauna. Science 313: 1429–1431.
5. Amano K, Kiel S (2007) Fossil vesicomyid bivalves from the North Pacific region. Veliger 49: 270–293.
6. Kaim A, Jenkins RG, Warén A (2008) Provannid and provannid-like gastropods from Late Cretaceous cold seeps of Hokkaido (Japan) and the fossil record of the Provannidae (Gastropoda: Abyssochrysoidea). Zool J Linn Soc 154: 421–436.
7. Kiel S, Amano K (2013) The earliest bathymodiolin mussels: Evaluation of Eocene and Oligocene taxa from deep-sea methane seep deposits in western Washington State, USA. J Paleont 87: 589–602.
8. Kaim A, Jenkins RG, Hikida Y (2009) Gastropods from Late Cretaceous hydrocarbon seep deposits in Omagari and Yasukawa, Nakagawa area, Hokkaido, Japan. Acta Palaeontol Pol 54: 463–690.
9. Campbell KA, Bottjer DJ (1995) Brachiopods and chemosymbiotic bivalves in Phanerozoic hydrothermal vent and cold seep environments. Geology 23: 321–324.
10. Gabb WM (1866–69) Cretaceous and Tertiary fossils. Calif Geol Surv Paleontol 2: 1–299.
11. Ascher E (1906) Die Gastropoden, Bivalven und Brachiopoden der Grodischter Schichten. Beitr Paläontol Geol Österreich-Ungarns Orients 19: 135–172.
12. Toula F (1911) Über Rhynchonella (Peregrinella Öhlert) multicarinata Lamk. sp. (1819) = Terebratula peregrina L. v. Buch (1833) von Zajzon bei Kronstadt. Abh kk Geol Reichsanst 20: 27–35.
13. Biernat G (1957) On *Peregrinella multicarinata* (Lamarck)(Brachiopoda). Acta Palaeontol Pol 2: 19–52.
14. Trümpy R (1956) Notizen zur mesozoischen Fauna der innerschweizerischen Klippen (I-II). Eclogae geol Helvetiae 49: 573–591.
15. Ager DV (1965) The adaptation of Mesozoic brachiopods to different environments. Palaeogeogr Palaeoclimatol Palaeoecol 1: 143–172.
16. Remeš M (1903) *Rhynchonella peregrina* bei Freiberg in Mähren. Verh kk geol Reichsanst 11: 223–225.
17. Macsotay O (1980) Molluscques benthiques du Crétacé inférieur. Une méthode de corrélation entre la Téthys mésogéenne et le domaine paléocaraïbe (Vénézuela). PhD thesis, Université Claude-Bernard, Lyon. 158 p.
18. Lemoine M, Arnaud-Vanneau A, Arnaud H, Létolle R, Mevel C, et al. (1982) Indices possibles de paléo-hydrothermalisme marin dans le Jurassique et le Crétacé des Alpes occidentales (océan téthysien et sa marge continentale européenne): essai d'inventaire. Bull Soc Géol France 24: 641–647.
19. Campbell KA, Bottjer DJ (1995) *Peregrinella*: an Early Cretaceous cold-seep-restricted brachiopod. Paleobiology 24: 461–478.
20. Sandy MR, Blodgett RB (1996) *Peregrinella* (Brachiopoda; Rhynchonellida) from the Early Cretaceous Wrangellia Terrane, Alaska. In: Copper P, Jin J, editors. Brachiopods. Rotterdam: A.A. Balkema. pp. 239–242.
21. Sun D (1986) Discovery of Early Cretaceous *Peregrinella* (Brachiopoda) in Xizang (Tibet) and its significance. Palaeontol Cathayana 2: 211–227.
22. Sandy MR (1995) A review of some Palaeozoic and Mesozoic brachiopods as members of cold seep chemosynthetic communities: "unusual" palaeoecology and anomalous palaeobiogeographic pattern explained. Földtani Közlöny 125: 241–258.
23. Sandy MR (2010) Brachiopods from ancient hydrocarbon seeps and hydrothermal vents. In: Kiel S, editor. The Vent and Seep Biota. Heidelberg: : Springer. pp. 279–314.
24. Gischler E, Sandy MR, Peckmann J (2003) *Ibergirhynchia contraria* (F.A. Roemer, 1850), an Early Carboniferous seep-related rhynchonellide brachiopod from the Harz Mountains, Germany-a possible successor to *Dzieduszyckia*? J Paleont 77: 293–303.
25. Peckmann J, Kiel S, Sandy MR, Taylor DG, Goedert JL (2011) Mass occurrences of the brachiopod *Halorella* in Late Triassic methane-seep deposits, Eastern Oregon. J Geol 119: 207–220.
26. Peckmann J, Campbell KA, Walliser OH, Reitner J (2007) A Late Devonian hydrocarbon-seep deposit dominated by dimerelloid brachiopods, Morocco. Palaios 22: 114–122.
27. Peckmann J, Sandy MR, Taylor DG, Gier S, Bach W (2013) An Early Jurassic brachiopod-dominated seep deposit enclosed by serpentinite, eastern Oregon, USA. Palaeogeogr Palaeoclimatol Palaeoecol 390: 4–16.
28. Short EJ, Snyder DC, Trop J, Hart WK, Layer PW (2005) New findings on Early Cretaceous volcanism within the allochthonous Wrangellia Terrane, south-central Alaska: stratigrpahic, geochronogic, and geochemical data from the Chisana Formation, Nutzotin Mountains. Geol Soc Am Abstr Program 37: 81.
29. Thieuloy J-P (1972) Biostratigraphie des lentilles a peregrinelles (Brachiopodes) de l'Hauterivien de Rottier (Drôme, France). Geobios 5: 5–53.
30. Kiel S (2013) Lucinid bivalves from ancient methane seeps. J Moll Stud 79: 346–363.
31. Bosellini A, Morsilli M (1997) A Lower Cretaceous downing unconformity on the eastern flank of the Apulia Platform (Gargano Promontory, southern Italy). Cret Res 18: 51–61.
32. Posenato R, Morsilli M (1999) New species of *Peregrinella* (Brachiopoda) from the Lower Cretaceous of the Gargano Promontory (southern Italy). Cret Res 20: 641–654.
33. Graziano R, Taddei Ruggiero E (2008) Cretaceous brachiopod-rich facies of the carbonate platform-to-basin transitions in southern Italy: stratigraphic and paleoenvironmental significance. Boll Soc Geol Ital 127: 407–422.
34. Boller K (1963) Stratigraphische und mikropaläontologische Untersuchungen in Neocom der Kippendecke (östlich der Rhone). Eclogae geol Helvetiae 56: 15–102.
35. Kiel S, Peckmann J (2008) Paleoecology and evolutionary significance of an Early Cretaceous *Peregrinella*-dominated hydrocarbon-seep deposit on the Crimean Peninsula. Palaios 23: 751–759.
36. Kiel S (2008) Parasitic polychaetes in the Early Cretaceous hydrocarbon seep-restricted brachiopod *Peregrinella multicarinata*. J Paleont 82: 1214–1216.
37. Peckmann J, Birgel D, Kiel S (2009) Molecular fossils reveal fluid composition and flow intensity at a Cretaceous seep. Geology 37: 847–850.
38. Berkland JO (1973) Rice Valley outlier - new sequence of Cretaceous-Paleocene strata in northern Coast Ranges, California. Geol Soc Am Bull 84: 2389–2406.
39. Campbell KA, Farmer JD, Des Marais D (2002) Ancient hydrocarbon seeps from the Mesozoic convergent margin of California: carbonate geochemistry, fluids and palaeoenvironments. Geofluids 2: 63–94.
40. Birgel D, Thiel V, Hinrichs K-U, Elvert M, Campbell KA, et al. (2006) Lipid biomarker patterns of methane-seep microbialites from the Mesozoic convergent margin of California. Org Geochem 37: 1289–1302.
41. Kiel S, Campbell KA, Elder WP, Little CTS (2008) Jurassic and Cretaceous gastropods from hydrocarbon-seeps in forearc basin and accretionary prism settings, California. Acta Palaeontol Pol 53: 679–703.
42. Sandy MR, Lazar I, Peckmann J, Birgel D, Stoica M, et al. (2012) Methane-seep brachiopod fauna within turbidites of the Sinaia Formation, Eastern Carpathian Mountains, Romania. Palaeogeogr Palaeoclimatol Palaeoecol 323–325: 42–59.
43. MacDonald IR (1998) Stability and change in Gulf of Mexico chemosynthetic communities: Interim Report. Prepared by the Geochemical and Environmental Research Group, Texas A&M University. U.S. Dept. of the Interior, Minerals Mgmt. Service, Gulf of Mexico OCS Region, New Orleans. 116 p.

44. Brooks JM, Fisher CR, Roberts HH, Bernard B, MacDonald IR, et al. (2009) Investigations of chemosynthetic communities on the lower continental slope of the Gulf of Mexico: Interim Report 2. U.S. Dept. of the Interior, Minerals Mgmt. Service, Gulf of Mexico OCS Region, New Orleans. 360 p.
45. Chryploff G (1958) Ein Fund von *Peregrinella* cf. *peregrina* d'Orbigny in der Unteren Kreide Norddeutschlands (Gebiet Werle in Mecklenburg). Z angew Geol 4: 70.
46. Brand U, Logan A, Hiller N, Richardson J (2003) Geochemistry of modern brachiopods: applications and implications for oceanography and paleoceanography. Chem Geol 198: 305–334.
47. Lear CH, Elderfield H, Wilson PA (2000) Cenozoic deep-sea temperatures and global ice volumes from Mg/Ca in benthic foraminiferal calcite. Science 287: 269–272.
48. McArthur JM (1994) Recent trends in strontium isotope stratigraphy. Terra Nova 6: 331–358.
49. Bailey TR, McArthur JM, Prince H, Thirlwall MF (2000) Dissolution methods for strontium isotope stratigraphy: whole rock analysis. Chem Geol 167: 313–319.
50. Reinhardt EG, Cavazza W, Patterson RT, Blenkinsop J (2000) Differential diagenesis of sedimentary components and the implication for strontium isotope analysis of carbonate rocks. Chem Geol 164: 331–343.
51. McArthur JM, Howarth RJ, Bailey TR (2001) Strontium isotope stratigraphy: LOWESS version 3: Best fit to the marine Sr-isotope curve for 0–509 Ma and accompanying look-up table for deriving numerical age. J Geol 109: 155–170.
52. McArthur JM, Howarth RJ, Shields GA (2012) Strontium isotope stratigraphy. In: Gradstein FM, Ogg JG, Schmitz M, Ogg G, editors. The Geologic Time Scale 2012. Elsevier. pp. 127–144.
53. Carroll M, Romanek CS (2008) Shell layer variation in trace element concentration for the freshwater bivalves *Elliptio complanata*. Geo-Mar Let 28: 369–381.
54. Nielsen SN, Glodny J (2009) Early Miocene subtropical water temperatures in the southeast Pacific. Palaeogeogr Palaeoclimatol Palaeoecol 280: 480–488.
55. Birgel D, Elvert M, Han X, Peckmann J (2008) ^{13}C-depleted biphytanic diacids as tracers of past anaerobic oxidation of methane. Org Geochem 39: 152–156.
56. Hammer Ø, Harper DAT, Ryan PD (2001) PAST: Palaeontological Statistics software package for education and data analysis. Palaeontol Electronica 4: 9 pp.
57. Paull CK, Chanton JP, Martens CS, Fullagar PD, Neumann AC, et al. (1991) Seawater circulation through the flank of the Florida platform: evidence and implications. Mar Geol 102: 265–279.
58. Aharon P, Schwarcz HP, Roberts HH (1997) Radiometric dating of submarine hydrocarbon seeps in the Gulf of Mexico. Geol Soc Am Bull 109: 568–579.
59. Anderson FM (1938) Lower Cretaceous deposits in California and Oregon. Geol Soc Am Spec Pap 16: 1–339.
60. Gabb WM (1869) Cretaceous and Tertiary fossils: Palaeontology, v. II. Geological Survey of California 1–299.
61. Campbell KA, Peterson D, Alfaro AC (2008) Two new species of *Retiskenea*? (Gastropoda: Neomphalidae) from Lower Cretaceous hydrocarbon seep-carbonates of northern California. J Paleont 82: 140–153.
62. Slaczka A, Kaminski MA (1998) A guidebook to excursions in the Polish Flysch Carpathians. Grzybowski Foundation Special Publication 6: 1–173.
63. Ortiz-Hernández LE, Acevedo-Sandoval OA, Flores-Castro K (2003) Early Cretaceous intraplate seamounts from Guanajuato, central Mexico: geochemical and mineralogical data. Rev Mex Sci Geol 20: 27–40.
64. Gradstein FM, Ogg JG, Schmitz M, Ogg G, Eds., *The Geologic Time Scale 2012* (Elsevier, 2012), pp. 1176.
65. Peckmann J, Thiel V (2004) Carbon cycling at ancient methane-seeps. Chem Geol 205: 443–467.
66. Graziano R (1999) The Early Cretaceous drowning unconformities of the Apulia carbonate platform (Gargano Promontory, southern Italy): local fingerprints of global palaeoceanographic events. Terra Nova 11: 245–250.
67. Kiel S, Campbell KA, Gaillard C (2010) New and little known mollusks from ancient chemosynthetic environments. Zootaxa 2390: 26–48.
68. Birgel D, Himmler T, Freiwald A, Peckmann J (2008) A new constraint on the antiquity of anaerobic oxidation of methane: Late Pennsylvanian seep limestones from southern Namibia. Geology 36: 543–546.
69. Goossens H, de Leeuw JW, Schenck PA, Brassell SC (1984) Tocopherols as likely precursors of pristane in ancient sediments and crude oils. Nature 312: 440–442.
70. Hayes JM, Strauss H, Kaufman AJ (1999) The abundance of ^{13}C in marine organic matter and isotopic fractionation in the global biogeochemical cycle of carbon during the past 800 Ma. Chem Geol 161: 103–125.
71. Campbell KA, Carlson C, Bottjer DJ (1993) Fossil cold seep limestones and associated chemosymbiotic macroinvertebrate faunas, Jurassic-Cretaceous Great Valley Group, California. In: Graham SA, Lowe DR, editors. Advances in the Sedimentary Geology of the Great Valley Group, Sacramento Valley, California. Los Angeles: Pacific Section of the Society of economic Paleontologists and Mineralogists. pp. 37–50.
72. Kiel S, Wiese F, Titus AL (2012) Shallow-water methane-seep faunas in the Cenomanian Western Interior Seaway: No evidence for onshore-offshore adaptations to deep-sea vents. Geology 40: 839–842.
73. Kiel S (2010) On the potential generality of depth-related ecologic structure in cold-seep communities: Cenozoic and Mesozoic examples. Palaeogeogr Palaeoclimatol Palaeoecol 295: 245–257.
74. Jenkins RG, Kaim A, Little CTS, Iba Y, Tanabe K, et al. (2013) Worldwide distribution of modiomorphid bivalve genus *Caspiconcha* in late Mesozoic hydrocarbon seeps. Acta Palaeontol Pol 58: 357–382.
75. Kaim A, Kelly SRA (2009) Mass occurrence of hokkaidoconchid gastropods in the Upper Jurassic methane seep carbonate from Alexander Island, Antarctica. Antarct Sci 21: 279–284.
76. Hammer Ø, Nakrem HA, Little CTS, Hryniewicz K, Sandy MR, et al. (2011) Hydrocarbon seeps close to the Jurassic-Cretaceous boundary, Svalbard. Palaeogeogr Palaeoclimatol Palaeoecol 306: 15–26.
77. Kiel S, Amano K, Jenkins RG (2008) Bivalves from Cretaceous cold-seep deposits on Hokkaido, Japan. Acta Palaeontol Pol 53: 525–537.
78. Kiel S, Birgel D, Campbell KA, Crampton JS, Schiøler P, et al. (2013) Cretaceous methane-seep deposits from New Zealand and their fauna. Palaeogeogr Palaeoclimatol Palaeoecol 390: 17–34.
79. Sahling H, Rickert D, Lee RW, Linke P, Suess E (2002) Macrofaunal community structure and sulfide flux at gas hydrate deposits from the Cascadia convergent margin, NE Pacific. MEPS 231: 121–138.
80. Newman WA, Yamaguchi T, Southward AJ (2006) Arthropoda, Crustacea, Cirripedia. Denisia 18: 359–368.
81. Sandy MR, Campbell KA (1994) New rhynchonellid brachiopod genus from Tithonian (Upper Jurassic) cold seep deposits of California and its paleoenvironmental setting. J Paleont 68: 1243–1252.
82. Sepkoski JJ (2002) A compendium of fossil marine animal genera. Bull Am Paleont 363: 1–563.
83. Sepkoski JJ (1998) Rates of speciation in the fossil record. Philosophical Transactions of the Royal Society of London B 353: 315–326.
84. Stanley SM (2007) An analysis of the history of marine animal diversity. Paleobiology 33: 1–55.
85. Thuy B, Kiel S, Dulai A, Gale AS, Kroh A, et al. (2014) First glimpse into Lower Jurassic deep-sea biodiversity: in-situ diversification and resilience against extinction. Proc Biol Sci 281: 20132624.
86. Pucéat E, Lécuyer C, Reisberg L (2005) Neodymium isotope evolution of NW Tethyan upper ocean waters throughout the Cretaceous. EPSL 236: 705–720.
87. Ager DV (1986) Migrating fossils, moving plates and an expanding Earth. Modern Geol 10: 377–390.
88. Bodin S, Godet A, Föllmi KB, Vermeulen J, Arnaud H, et al. (2006) The late Hauterivian Faraoni oceanic anoxic event in the western Tethys: Evidence from phosphorus burial rates. Palaeogeogr Palaeoclimatol Palaeoecol 235: 245–264.
89. Cordes EE, Bergquist DC, Fisher CR (2009) Macro-ecology of Gulf of Mexico cold seeps. Ann Rev Mar Sci 1: 143–168.
90. Van Dover CL (2000) The ecology of deep-sea hydrothermal vents. Princeton: Princeton University Press. 424 p.
91. Niemann H, Fischer D, Graffe D, Knittel K, Montiel A, et al. (2009) Biogeochemistry of a low-activity cold seep in the Larsen B area, western Weddell Sea, Antarctica. Biogeosciences 6: 2383–2395.
92. Luff R, Wallmann K (2003) Fluid flow, methane fluxes, carbonate precipitation and biogeochemical turnover in gas hydrate-bearing sediments at Hydrate Ridge, Cascadia Margin: Numerical modeling and mass balances. Geochim Cosmochim Acta 67: 3403–3421.
93. Birgel D, Peckmann J (2008) Aerobic methanotrophy at ancient marine methane seeps: A synthesis. Org Geochem 39: 1659–1667.
94. Little CTS, Herrington RJ, Haymon RM, Danelian T (1999) Early Jurassic hydrothermal vent community from the Franciscan Complex, San Rafael Mountains, California. Geology 27: 167–170.
95. Thayer CW (1981) Ecology of living brachiopods. In: Broadhead TW, editor. Lophophorates. Notes for a Short Course. Knoxville: University of Tennessee. pp. 110–126.
96. Manceñido MO, Owen EF (2001) Post-Palaeozoic Rhynchonellida (Brachiopoda): classification and evolutionary background. In: Brunton CH, Cocks LRM, Long SL, editors. Brachiopods Past and Present. The Systematics Association, Special Volume series 63. London and New York: Taylor and Francis. pp. 189–200.
97. Lazar I, Panaiotu CE, Grigore D, Sandy MR, Peckmann J (2011) An unusual brachiopod assemblage in a Late Jurassic (Kimmeridgian) stromatactis mud-mound of the Eastern Carpathians (Haghimas Mountains), Romania. Facies 57: 627–647.
98. Scotese CR (2004) A continental drift flipbook. J Geol 112: 729–741.
99. Keenan KE (2010) Hydrocarbon seeps of the Mesozoic Great Valley Group forearc strata and Franciscan Complex, northern and central California, U.S.A. PhD thesis, University of California, Riverside. 273 p.
100. Amano K, Jenkins RG, Hikida Y (2007) A new gigantic *Nucinella* (Bivalvia: Solemyoida) from the Cretaceous cold-seep deposit in Hokkaido, northern Japan. Veliger 49: 84–90.
101. Kaim A, Jenkins RG, Tanabe K, Kiel S (2014) Mollusks from late Mesozoic seep deposits, chiefly in California. Zootaxa. 3861: 401–440
102. Renngarten V (1924) O Kavkaykikh Peregrinellae (Sur les Pérégrinelles du Caucase). Izvestiia Geol Komiteta, Leningrad 42: 119–128.
103. Gaillard C, Rio M, Rolin Y (1992) Fossil chemosynthetic communities related to vents or seeps in sedimentary basins: the pseudobioherms of southeastern France compared to other world examples. Palaios 7: 451–465.
104. Kelly SRA, Ditchfield PW, Doubleday PA, Marshall JD (1995) An Upper Jurassic methane-seep limestone from the Fossil Bluff Group forearc basin of Alexander Island, Antarctica. J Sediment Res A65: 274–282.

105. Stanton TW (1895) Contributions to the Cretaceous paleontology of the Pacific coast: the fauna of the Knoxville beds. US Geol Surv Bull 133: 1–132.
106. Kaim A, Skupien P, Jenkins RG (2013) A new Lower Cretaceous hydrocarbon seep locality from Czech Carpathians and its fauna. Palaeogeogr Palaeoclimatol Palaeoecol 390: 42–51.
107. Kelly SRA, Blanc E, Price SP, Withham AG (2000) Early Cretaceous giant bivalves from seep-related limestone mounds, Wollaston Forland, Northeast Greenland. In: Harper EM, Taylor JD, Crame JA, editors. The evolutionary biology of the Bivalvia. London: Geological Society of London, Special Publication. pp. 227–246.
108. Agirrezabala LM, Kiel S, Blumenberg M, Schäfer N, Reitner J (2013) Outcrop analogues of pockmarks and associated methane-seep carbonates: a case study from Lower Cretaceous (Albian) of the Basque-Cantabrian Basin, western Pyrenees. Palaeogeogr Palaeoclimatol Palaeoecol 390: 94–115.
109. Nobuhara T, Onda D, Kikuchi N, Kondo Y, Matsubara K, et al. (2008) Lithofacies and fossil assemblages of the Upper Cretaceous Sada Limestone, Shimanto City, Kochi Prefecture, Shikoku, Japan. Fossils Palaeont Soc Japan 84: 47–60.
110. Jenkins RG, Kaim A, Hikida Y, Tanabe K (2007) Methane-flux-dependent lateral faunal changes in a Late Cretaceous chemosymbiotic assemblage from the Nakagawa area of Hokkaido, Japan. Geobiology 5: 127–139.